The Eigensolutions of the Linearized Balance Equations over a Sphere

ANTONIO D. MOURA[1]

Department of Meteorology, Massachusetts Institute of Technology, Cambridge 02139

(Manuscript received 16 May 1975, in revised form 25 February 1976)

ABSTRACT

Solutions of the linearized balance equations over a sphere are presented and compared with the Laplace's tidal equations results obtained by Longuet-Higgins. On these lines, this study searches for a partial answer concerning the accuracy of the balance system for describing slow, large-scale motions in the atmosphere. The solutions corresponding to Hough's second class waves [small values of $\epsilon=(2\Omega a)^2/c^2$] are well described by the balance system. At large values of ϵ there are apparent discrepancies for the Rossby symmetric modes as compared to Longuet-Higgins type 2 solutions. Nevertheless, for the antisymmetric modes the agreement is good. The linearized version of the motions studied by Burger is also a solution of the balance equations, corresponding to small frequencies and negative values of ϵ. There are also unrealistic solutions (in the light of the balance approximation) with high frequencies and $\epsilon<0$.

An integral theorem shows that for $\epsilon>0$ only westward propagating waves are solutions of the balance system. In particular, it shows that the equatorial Kelvin wave is not a solution. The westward propagating part of the mixed Rossby-gravity mode is a solution, but with slightly higher frequency when compared to Longuet-Higgins' results.

A study of the "modified balance" equations derived by Charney shows that they describe well all the equatorial Rossby modes. They also describe the equatorial Kelvin wave at large values of ϵ. Unfortunately, they have additional unrealistic high-frequency eastward-propagating free wave solutions. An interative numerical method is suggested in the hope of avoiding these spurious solutions.

A two-layer spherical model is used to study the instability properties of a basic state of solid rotation. It shows that the balance and the quasi-geostrophic equations have unstable solutions which are remarkably alike for realistic values of the parameters involved.

1. Introduction

The balance equations are a simplified set of meteorological equations in which the divergence equation is replaced by a dignostic relationship between the horizontal nondivergent velocity and the horizontal variations in the pressure field. This is on the assumption that, for large-scale motions, the horizontal divergence is much smaller than the vertical component of the vorticity. They are suitable for treating motions without gravity waves, but are able to treat more general type of motions than the quasi-geostrophic relation.

These equations appear in the works of Charney (1955) and Bolin (1955) and have been used in global models of the atmosphere where the mid-latitude β-plane gives unacceptable results (Bryan, 1959; Peng, 1965; Clark, 1970; Cunnold *et al.*, 1975). They are obtained as a second-order approximation in the expansion of the primitive equations in terms of the Rossby number (Charney, 1962, 1973; Monin, 1952, 1958). Charney's (1962, 1973) derivation is a more rigorous one, and shows that the expansion holds even for $\mathrm{Ro}=O(1)$ if the Richardson number (Ri) is large enough that $(\mathrm{RiRo})^{-1}$ remains small.

Lorenz (1960) has shown in a very enlightening manner that the equations form an energetically consistent set. He is able to derive the balance equations by means of a systematic and consistent omission of certain terms in the primitive equations. The equation of balance has been used in the context of obtaining the initial set of data required to solve a well-posed initial-boundary-value problem for the equations describing the large-scale motions in dynamic meteorology (Charney, 1955; Phillips, 1960).

Because the equations do not treat gravity waves, they may be integrated through a numerical scheme with larger time steps, which is a highly desirable feature when lengthy integrations have to be performed (e.g., in a general circulation model).

The equations, however, form a highly implicit set, which makes their study difficult. Charney (1962) has numerically integrated them through an iterative process, the convergence of which requires the potential vorticity to be positive throughout the region of integration. He argues that this criterion for convergence holds even when the ellipticity condition for the Monge-

[1] On leave from and presently at Instituto de Pesquisas Espaciais, 12200 São José dos Campos, São Paulo, Brazil.

Ampere equation (Bolin, 1955; Miyakoda, 1960; Houghton, 1968) is not satisfied.

We want to consider the following question: *How accurate is the balance system for describing slow, large-scale motions in the atmosphere?* To partly answer this question, we look at linear solutions of the balance system on a sphere, and compare them with the more fundamental linear solutions for the Laplace tidal equations (referred to henceforth as LTE) obtained by Longuet-Higgins (1968). In general, we will make use of numerical methods for the solution of this problem, accompanied with analytical solutions to some asymptotic cases.

The balance system is briefly described in Section 2, where we also treat the linearization of the equations, with respect to a resting basic state. The latter allows for the separation of horizontal and vertical structures of the equations. A summary of the solutions to the LTE is presented in Section 3, with special attention to the asymptotic solutions. Here we have attempted to illustrate compactly the eigenvalues of the LTE in one figure (Fig. 1).

In Section 4, the eigenvalue-eigenfunction problem is formulated for the balance equations and an integral theorem is derived. The latter shows that the equatorial Kelvin wave of the LTE is not a solution of the balance equations. Numerical solutions and some asymptotic studies of the eigenvalue problem are compared with the LTE results. Eigenfunctions for some selected modes are shown in Section 5 to describe their variation with latitude and the parameters involved.

In Section 6 we present a study of baroclinic stability using a simple family of zonal wind profiles $\{\bar{U}=a\alpha(p)\cos(\text{lat})[1+\delta\sin^2(\text{lat})]\}$ in a two-layer model. Here we compare the solutions described by the balance equations and the quasi-geostrophic equations, using realistic values of the parameters involved.

In an attempt to find a better description for the equatorial Rossby modes as described by the balance equations, we consider in Section 7 the inclusion of the "$\beta(\partial\chi/\partial x)$" term in the equation of balance. The resulting set of equations is denoted as the "modified balance equations" and also forms an energetically consistent set. These equations are found in the work of Charney (1962) but are even more difficult to solve numerically than are the balance equations.

2. Linear problem for resting state

Since we intend to verify how well the slow motions are described by the balance system, a comparative parallel study of the primitive and balance equations seems to be the appropriate approach to the problem.

We now formulate the equations using indices (α,α') and braces $(\{\ \})$ to indentify simplifications to be made in order to get the balance system.

The hydrostatic forms of the vorticity, divergence, thermodynamic and continuity equations using $Z=-\ln(p/p_0)$ are (Phillips, 1973)

$$\nabla^2\partial\psi/\partial t=-\hat{\mathbf{k}}\times\nabla\psi\cdot\nabla(\zeta+f)-\nabla\cdot(\zeta+f)\nabla\chi-\nabla\cdot(\dot{Z}\nabla\partial\psi/\partial Z)+\{\nabla\cdot(\dot{Z}\hat{\mathbf{k}}\times\nabla\partial\chi/\partial Z)\}-\nabla\cdot(\hat{\mathbf{k}}\times\mathbf{F}),\quad(2.1)$$

$$\alpha'(\nabla^2\partial\chi/\partial t)=-\nabla^2(\Phi+\nabla\psi\cdot\nabla\psi/2)+\nabla\cdot(\zeta+f)\nabla\psi-\alpha(\hat{\mathbf{k}}\times\nabla\chi\cdot\nabla f)-\{\nabla^2(\nabla\chi\cdot\nabla\chi/2+\nabla\psi\cdot\nabla\chi)+\nabla\cdot(\dot{Z}\nabla\partial\chi/\partial Z)+\hat{\mathbf{k}}\times\nabla\chi\cdot\nabla\zeta-\hat{\mathbf{k}}\cdot\nabla\dot{Z}\times\nabla\partial\psi/\partial Z-\nabla\cdot\mathbf{F}\},\quad(2.2)$$

$$\partial^2\Phi/\partial t\partial Z=-(\hat{\mathbf{k}}\times\nabla\psi+\nabla\chi)\cdot\nabla(\partial\Phi/\partial Z)-S\dot{Z}+\mathcal{R}q/C_p,\quad(2.3)$$

$$\nabla^2\chi=-(\partial/\partial Z-1)\dot{Z},\quad(2.4)$$

where

$$S=-(p^2/\rho)\partial\ln\Theta/\partial p=(\mathcal{R}TN/g)^2,\quad(2.5)$$

is the static stability and ∇ the horizontal del operator in spherical coordinates (a list of symbols is presented in Appendix A).

The lower boundary condition is obtained by applying

$$\dot{Z}=-(\mathcal{R}T)^{-1}[\partial\Phi/\partial t+(\hat{\mathbf{k}}\times\nabla\psi+\nabla\chi)\cdot\nabla\Phi-gW]\quad(2.6)$$

at the ground; $\dot{Z}$ is $p^{-1}(dp/dt)=-\tilde{\omega}/p$ and the equations without simplification have the indices (α,α') all equal to 1.

a. The balance system of equations

The simplification which leads to the so-called balance equations is obtained by omitting the terms in braces and letting $\alpha'=0$ with $\alpha=0$ or 1 in (2.1) and (2.2). This forms an energy preserving system (Lorenz, 1960; Charney, 1962) if $\mathbf{F}=q=0$ and $\tilde{\omega}=0$ at $p=0$ and $p=p_0$, and is correct up to two orders in the Rossby number expansion of the quasi-geostrophic system on a mid-latitude β-plane (Monin, 1958; Charney, 1962). (Charney retains the $\alpha=1$ term. This is energetically consistent but it is a small term in the quasi-geostrophic expansion.)

For future reference we now specialize to the balance equations:

$$\nabla^2\partial\psi/\partial t=-\hat{\mathbf{k}}\times\nabla\psi\cdot\nabla(\zeta+f)-\nabla\cdot(\zeta+f)\nabla\chi-\underline{\nabla\cdot(\dot{Z}\nabla\partial\psi/\partial Z)}-\nabla\cdot(\hat{\mathbf{k}}\times\mathbf{F}),\quad(2.7)$$

$$\nabla^2\Phi=\nabla\cdot f\nabla\psi+\underline{\nabla\cdot[\zeta\nabla\psi-\nabla(\nabla\psi\cdot\nabla\psi/2)]}-\alpha(\nabla f\cdot\hat{\mathbf{k}}\times\nabla\chi),\quad(2.8)$$

$$\partial^2\Phi/\partial t\partial Z=-(\hat{\mathbf{k}}\times\nabla\psi+\nabla\chi)\cdot\nabla(\partial\Phi/\partial Z)-S\dot{Z}+\mathcal{R}q/C_p,\quad(2.9)$$

$$\nabla^2\chi=-(\partial/\partial Z-1)\dot{Z},\quad(2.10)$$

$$\dot{Z}=-(\mathcal{R}T)^{-1}[\partial\Phi/\partial t+(\hat{\mathbf{k}}\times\nabla\psi+\nabla\chi)\cdot\nabla\Phi-gW],\quad(2.11)$$

at the ground. The cases $\alpha=0$ or 1 will be referred to respectively as the "balance" or "modified balance" system. The nonlinear underlined terms in (2.7) and (2.8) can be omitted together without violating conservation of energy. This option is examined in Section 6. Under special choices of the basic state it is possible to separate out the vertical and horizontal dependence of the equations.

Later (Section 6) we shall consider a zonal basic flow (nonzero) bearing some resemblance to the atmosphere, but now we will analyze the equations describing hydrostatic perturbations in a resting, stratified atmosphere without heating and friction over a spherical rotating earth. What we have in mind is to compare, whenever possible, the eigensolutions of the balance system with those of the hydrostatic equations resulting from the thorough study by Longuet-Higgins (1968). In this linearized homogeneous problem, Eqs. (2.1)–(2.6) become

$$\nabla^2\partial\psi'/\partial t=-(2\Omega a^{-2})\partial\psi'/\partial\phi-2\Omega\mu\nabla^2\chi' -(2\Omega a^{-2})(1-\mu^2)\partial\chi'/\partial\mu, \quad (2.12)$$

$$\alpha'(\nabla^2\partial\chi'/\partial t)+\nabla^2\Phi'=2\Omega\mu\nabla^2\psi'+(2\Omega a^{-2})(1-\mu^2)\partial\psi'/\partial\mu -\alpha(2\Omega a^{-2})\partial\chi'/\partial\phi, \quad (2.13)$$

$$\partial^2\Phi'/\partial t\partial Z=-\bar{S}(Z)\dot{Z}', \quad (2.14)$$

$$\nabla^2\chi'=-(\partial/\partial Z-1)\dot{Z}', \quad (2.15)$$

with the lower boundary condition (taking $W=0$)

$$\dot{Z}'=-(\Re\bar{T})^{-1}\partial\Phi'/\partial t \quad \text{at} \quad Z=0, \quad (2.16)$$

and where

$$a^2\nabla^2\equiv(\partial/\partial\mu)[(1-\mu^2)\partial/\partial\mu]+(1-\mu^2)^{-1}\partial^2/\partial\phi^2 \quad (2.17)$$

is the horizontal part of the spherical Laplacian operator, ϕ is longitude and $\mu=\sin(\text{latitude})$. The primes indicate perturbation quantities and an overbar means basic state. The balance system in this linearized form is obtained by making $\alpha'=0$ and $\alpha=0$ ($\alpha=1$ will be discussed in Section 7). The general problem ($\alpha'=\alpha=1$) is a very important one for both atmospheric and oceanic motions. The general equations arise in the study of tides, the theory of which was originally formulated by Laplace [Lamb, 1932 (pp. 330 and 554); Taylor, 1936]. The influence of the nonlinear terms does not appear in the present formulation, which restricts the scope and significance of our analysis.

b. Horizontal and vertical structure

In order to separate out the vertical and horizontal structures we search for solutions of the form

$$\left.\begin{aligned}(\psi',\chi',\Phi')&=(\psi,\chi,\Phi)(\phi,\mu,t)A(Z)\\ \dot{Z}'&=W(\phi,\mu,t)B(Z)\end{aligned}\right\}. \quad (2.18)$$

It can be shown (Phillips, 1973) that when (2.18) is put into (2.12)–(2.15) one obtains

$$a^2\nabla^2\partial\psi/\partial t=-2\Omega\partial\psi/\partial\phi-2\Omega\mu a^2\nabla^2\chi -2\Omega(1-\mu^2)\partial\chi/\partial\mu, \quad (2.19)$$

$$\alpha'(a^2\nabla^2\partial\chi/\partial t)=-a^2\nabla^2\Phi+2\Omega\mu a^2\nabla^2\psi+2\Omega(1-\mu^2)\partial\psi/\partial\mu -\alpha(2\Omega\partial\chi/\partial\phi), \quad (2.20)$$

$$\partial\Phi/\partial t=-c^2\nabla^2\chi. \quad (2.21)$$

Here c^2 is a separation constant and has dimensions of (velocity)^2.

The equations describing the horizontal structure are (2.19), (2.20) and (2.21).

The vertical structure is dependent upon the mean temperature $\bar{T}(Z)$ and is given by

$$d^2D(Z)/dZ^2+[\bar{S}(Z)/c^2-\tfrac{1}{4}]D(Z)=0. \quad (2.22)$$

The vertical structure also depends upon the thermal forcing that would appear in the right-hand side of (2.22) in the case of a forced problem. This equation is subject to the lower boundary condition

$$[dD/dZ+(\Re\bar{T}/c^2-\tfrac{1}{2})D]_{Z=0}=0, \quad (2.23)$$

where $D(Z)=B(Z)\exp(-Z/2)$, to determine the vertical structure. The upper boundary condition on $D(Z)$ is either that energy density be finite as $Z\to\infty$ or an imposed outward radiation condition as $Z\to\infty$ requiring the energy flux to be upward. Discussions concerning the upper boundary condition may be found in Lindzen (1967), Chapman and Lindzen (1970), and Eliassen and Palm (1960).

3. Tidal theory: A summary

In this section we will present a summary of the study of the LTE by Longuet-Higgins (1968). This summary is needed for a comparison with the results obtained for the linearized balance equations.

a. The tidal equations

It is our primary interest to study thoroughly the latitudinal structure of Eqs. (2.19), (2.20) and (2.21). In order to do so, we look for solutions of the form

$$(\psi,\chi,\Phi)(\phi,\mu,t) =\mathrm{Re}\{[P(\mu),iQ(\mu),2\Omega R(\mu)]\exp(is-i\sigma t)\}. \quad (3.1)$$

The latitudinal dependence of those equations is then

$$-\lambda\mathfrak{L}(P)+\mu\mathfrak{L}(Q)+(1-\mu^2)dQ/d\mu+sP=0, \quad (3.2)$$

$$\mu\mathfrak{L}(P)+(1-\mu^2)dP/d\mu+\alpha(sQ) =\mathfrak{L}(R)+\alpha'[\lambda\mathfrak{L}(Q)], \quad (3.3)$$

$$\mathfrak{L}(Q)=\lambda\epsilon R, \quad (3.4)$$

where $\lambda=\sigma/2\Omega$ is a nondimensional frequency, $\epsilon=4\Omega^2a^2/c^2$ a nondimensional parameter (called Lamb's parameter), and

$$\mathfrak{L}(\ )\equiv\{d[(1-\mu^2)d/d\mu]/d\mu-(1-\mu^2)^{-1}s^2\}(\ ).$$

Eqs. (3.2)–(3.4) with $\alpha'=\alpha=1$ are referred to as LTE

and form an eigenvalue-eigenfunction problem (Longuet-Higgins, 1968). The eigenvalue λ is real and its spectrum depends on the separation constant c^2 (or ϵ), on the longitudinal wavenumber s, and on a latitudinal modal number n, i.e.,

$$\lambda=\lambda(\epsilon,s,n). \tag{3.5}$$

In the case of a homogeneous ocean of depth h one gets the same equations but with $c^2=gh$. [This analogy has lead to the definition of the so-called "equivalent depth" of the atmosphere; Taylor (1936).] The eigenfunctions of the LTE are called Hough Functions on account of the important contribution made by Hough (1898) (Flattery, 1967; Lindzen, 1966, 1967, 1971).

The complete set of eigenfunctions in which a given forcing function can be expanded includes both positive and negative values of ϵ. Negative values of ϵ are needed in some forced problems [e.g., study of diurnal pressure oscillation resulting from insolation; Lindzen (1966)]. The discovery of these negative equivalent depth modes and their importance has been stressed by Lindzen (1966, 1971) [see also Dikii (1965) and Kato (1966)].

One example on the use of the eigenfunctions in a low-latitude forced problem (only $\epsilon>0$ modes are needed) is given by Matsuno (1966).

b. The eigenvalues of Laplace's tidal equations

Fig. 1 displays the general nature of the eigenvalues of LTE as derived by Longuet-Higgins (1968). For each fixed mode the surface $n=n(\epsilon,\lambda,s)$ is shown as a function of ϵ, the frequency λ, and the wavenumber s. (Strictly speaking, the values that s assumes are discrete.) The frequency ranges over $0<\lambda<\infty$ for positive ϵ but only over $0<\lambda<1$ for negative ϵ.

Fig. 2 represents a cross section of Fig. 1 at $\epsilon=100$ and shows the relationship between λ and s. In this figure, where the various modes are indicated, the "mixed Rossby-gravity mode" is seen to behave either like a Rossby mode or like a gravity mode for large negative or large positive values of s, respectively. For small values of s it has a mixed character (Matsuno, 1966).

Figs. 3, 4 and 5 (sections of Fig. 1) show the dependence of the frequency on the parameter ϵ for fixed values of s (0, 1, -1).

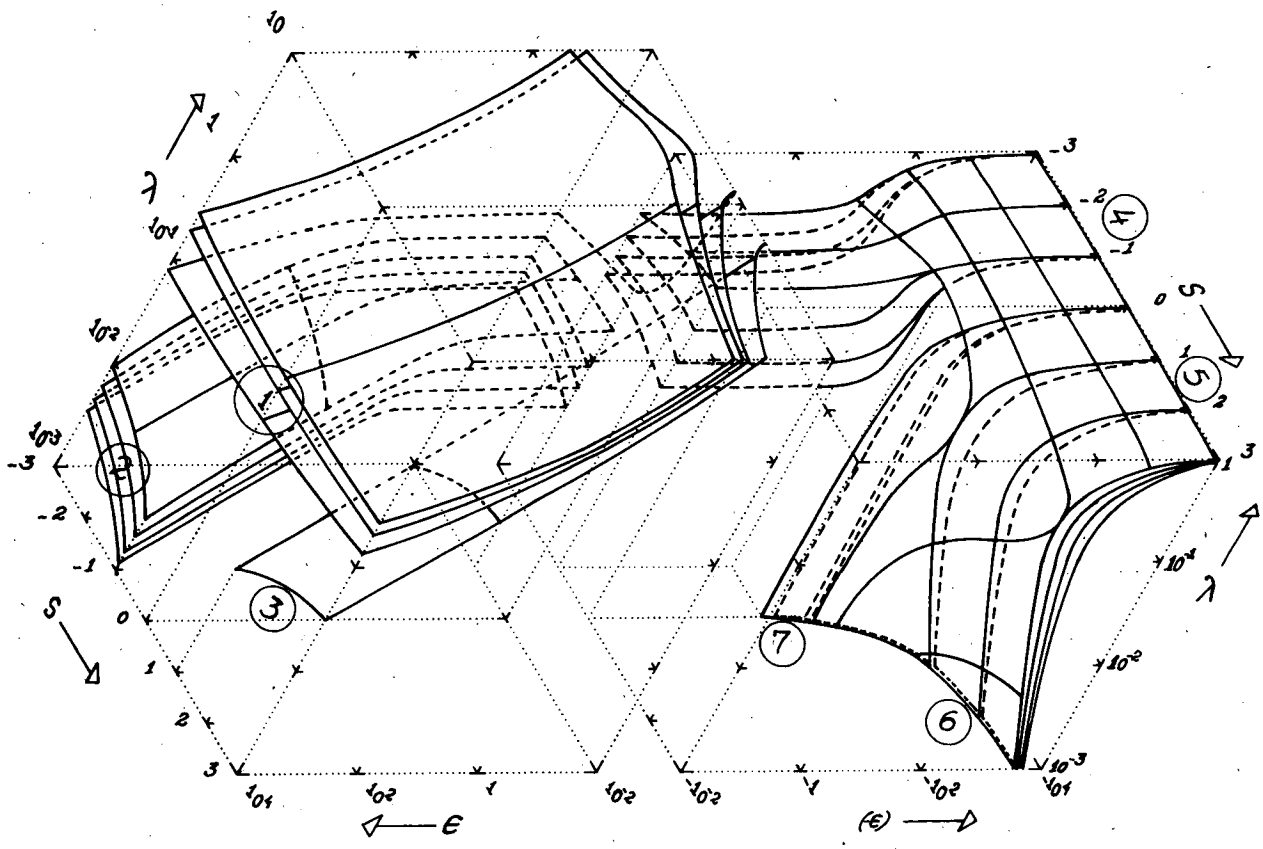

FIG. 1. Eigenvalues for Laplace's tidal equations constructed from the analysis by Longuet-Higgins. Surfaces are shown for selected latitudinal modes, as a functions of frequency ($\lambda>0$, on a log scale), longitudinal wavenumber (s), and Lamb's parameter ($\epsilon=4\Omega^2a^2/c^2$, also on a log scale). The encircled numbers refer to the seven limiting types described by Longuet-Higgins. Surfaces are drawn by continuity as if s could assume non-integer values except when the connection between $s=0$ and $s=1$ is not obvious.

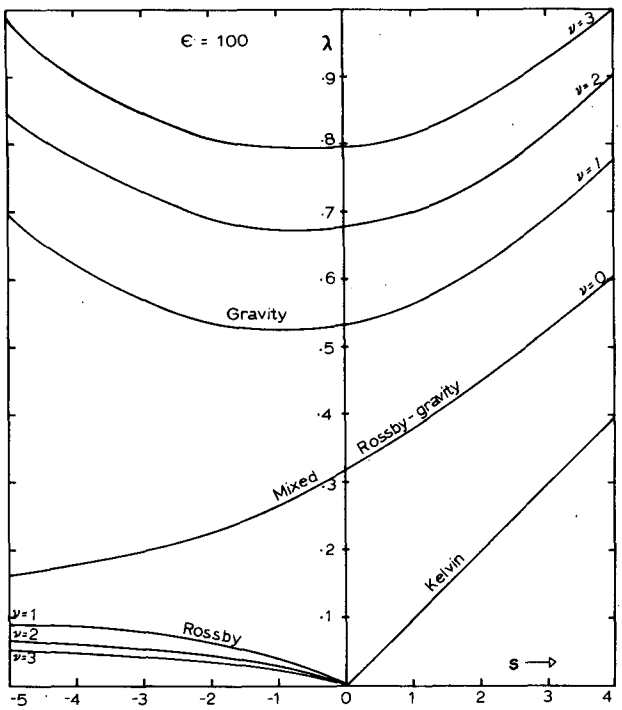

FIG. 2. Eigenvalues for Laplace's tidal equations for $\epsilon(=4\Omega^2a^2/c^2)=100$. The frequency ($\lambda$) dependence on the longitudinal wavenumber (s) is shown for selected modes, as indicated in the figure.

c. Asymptotic solutions

The eigenvalues shown in Fig. 1 are a result of numerical calculations when P, Q and R are expressed as series of surface spherical harmonics. The computations have revealed several asymptotic forms taken by the eigensolutions (Longuet-Higgins, 1968).

1) ASYMPTOTIC SOLUTIONS AS $\epsilon \to 0$

As $\epsilon \to +0$ the solutions separate out into two families:

Waves of the first class (gravity waves)

$$\lambda=\{n(n+1)/\epsilon\}^{\frac{1}{2}}, \quad n=|s|+\nu, \quad \nu=0, 1, 2, \ldots$$

Waves of the second class [nondivergent Rossby waves; Rossby (1939) and Haurwitz (1940)]

$$\lambda=-s/\{n(n+1)\}=-s/\{s^2-s(2\nu+1)+\nu(\nu+1)\}; \quad s<0, \nu=0, 1, 2, \ldots$$

The first family corresponds to irrotational motions with eigenfunctions given by $P(\mu)=0$ and $Q(\mu) \propto P_n^{|s|}(\mu)$, whereas the second family corresponds to nondivergent motions with $Q(\mu)=0$ and $P(\mu) \propto P_n^{-s}(\mu)$. Here $P_n^s(\mu)$ is the associated Legendre function of degree n and order s [Korn and Korn (1968), p. 870]. These results are found in the work of Hough (1898).

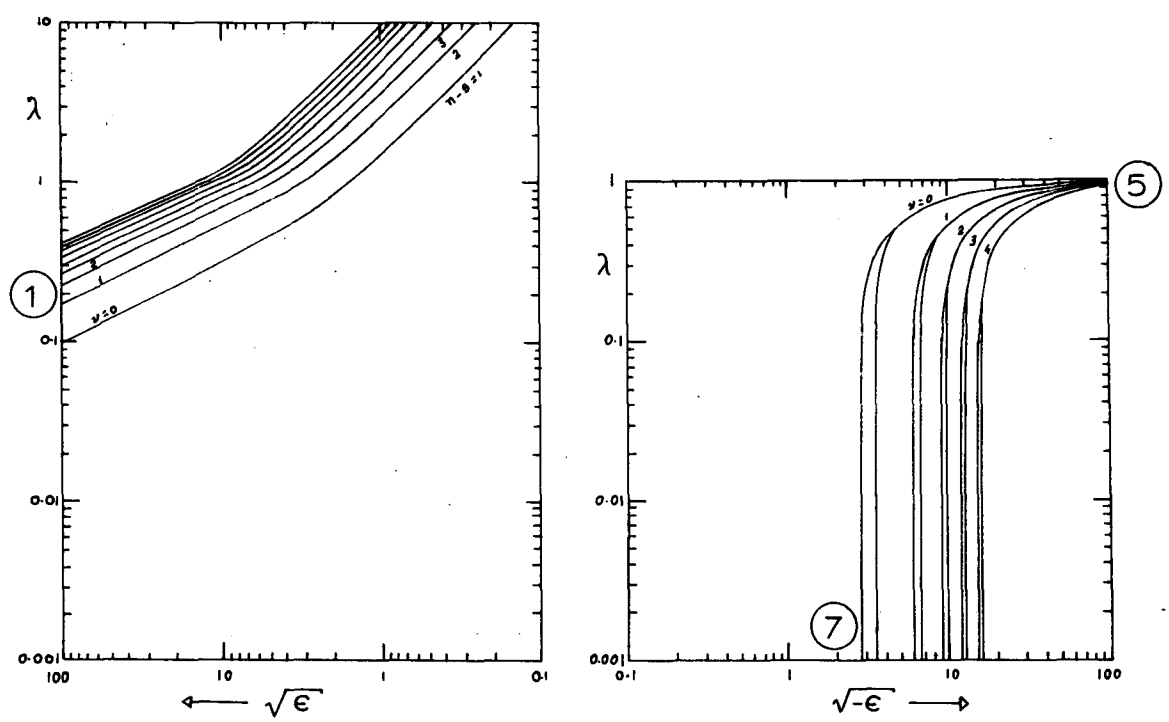

FIG. 3. Eigenvalues for Laplace's tidal equations for the longitudinal wavenumber $s=0$ constructed from the analysis by Longuet-Higgins. The frequency (λ) dependence on the parameter $\epsilon=4\Omega^2a^2/c^2$ is shown. The frequency is less than one for all negative values of ϵ. The encircled numbers refer to the limiting types described by Longuet-Higgins.

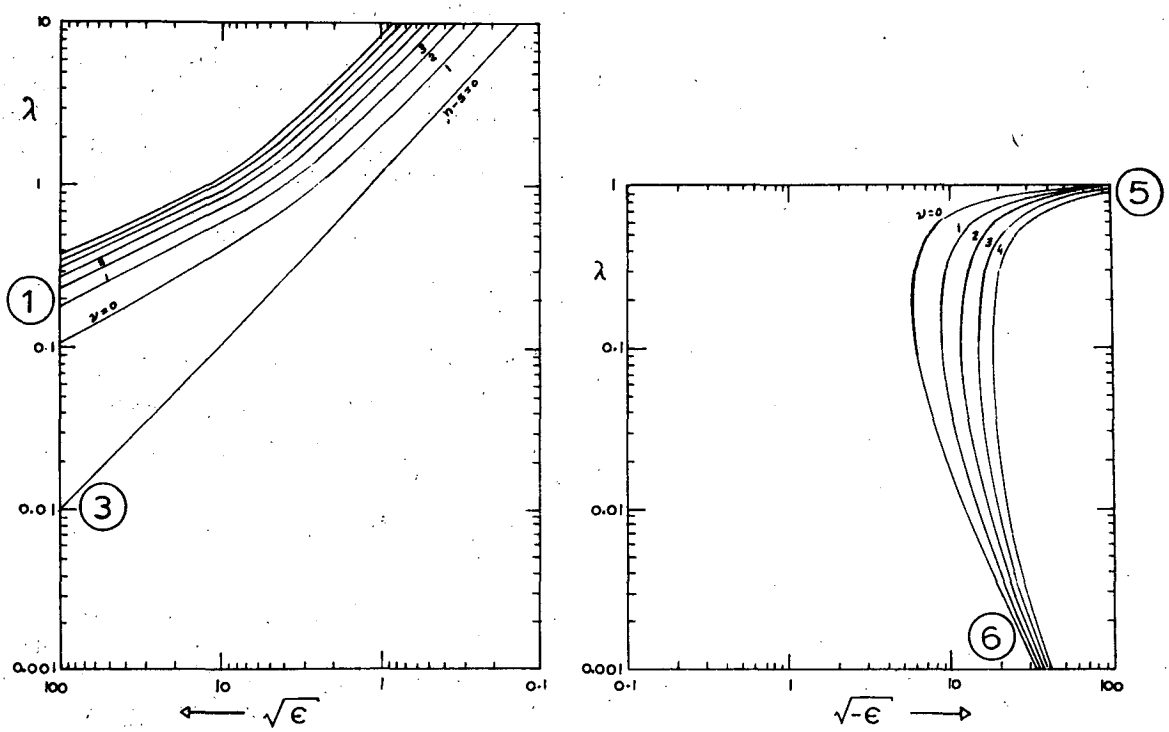

FIG. 4. As in Fig. 3 except for the longitudinal wavenumber $s=1$.

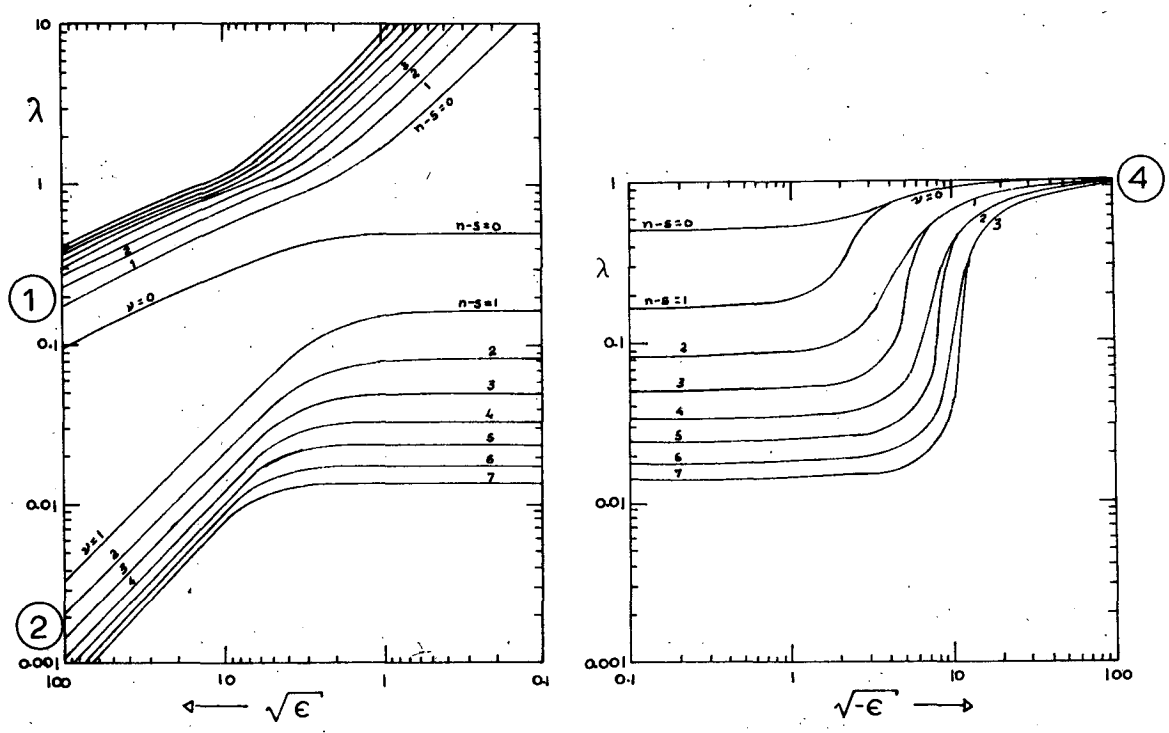

FIG. 5. As in Fig. 3 except for the longitudinal wavenumber $s=-1$.

As $\epsilon \to -0$ the only limiting forms of solutions correspond to a continuation of the waves of the second class.

2) ASYMPTOTIC SOLUTIONS AS $\epsilon \to +\infty$

The solutions comprise three types of motions, all of which are described in terms of Hermite functions. They are confined to the equatorial region as $\epsilon \to +\infty$, and as such were first described by Matsuno (1966). The Hermite functions [Jeffreys and Jeffreys (1972), p. 620] and the dispersion relation (a cubic equation for λ) appear as a result of the boundary conditions imposed on a parabolic cylinder equation for the meridional velocity, with exception of type 3.

Type 1: The motions of type 1 are inertial gravity waves with frequencies

$$\lambda=[(2\nu+1)^{\frac{1}{2}}]/\epsilon^{\frac{1}{2}}+s/[2(2\nu+1)\epsilon^{\frac{1}{2}}];\ \nu=0, 1, 2\ ,\ldots,$$

$s=0$, $s>0$, or $s<0$. The $\nu=0$ mode is referred to as the mixed Rossby-gravity mode with properties already mentioned. The associated meridional velocities are

$$v(\eta)=-i\exp(-\eta^2/2)H_\nu(\eta);\ \eta=\epsilon^{\frac{1}{4}}\mu,\ \nu=0, 1, 2, \ldots, \quad (3.6)$$

where $v(\mu)=i\{(1-\mu^2)dQ/d\mu+sP\}\{(1-\mu^2)^{-\frac{1}{2}}\}/a$ is the latitudinal dependence of the meridional velocity.

Type 2: These correspond to equatorially trapped westward propagating Rossby waves with frequencies given by

$$\lambda=-s/[(2\nu+1)\epsilon^{\frac{1}{2}}];\ \nu=1, 2, 3, \ldots, s<0,$$

and the meridional velocities described by

$$v(\eta)=-i\exp(-\eta^2/2)H_\nu(\eta). \quad (3.7)$$

{Note: The well-known decrease of Rossby wave frequencies with large $(-s)$ is not shown by the above formula for λ, as described by Longuet-Higgins. An expansion in powers of $\epsilon^{-\frac{1}{2}}$ to the next order replaces $(2\nu+1)\epsilon^{\frac{1}{2}}$ in the denominator by $(2\nu+1)\epsilon^{\frac{1}{2}}+s^2[1-(2\nu+1)^{-2}]-\frac{1}{4}(2\nu^2+2\nu-1)$.

Type 3: This represents a "Kelvin wave" solution propagating eastward along the equator with very small meridional velocity. Kelvin waves propagate along coastal boundaries in rotating systems with constant Coriolis parameter, and the change of sign of the Coriolis parameter on the equator here plays the role of an "equatorial wall" for this Kelvin wave solution. The zonal velocity is geostrophically balanced and has a Gaussian profile. The frequency is given by

$$\lambda=s[1+1/(4\epsilon^{\frac{1}{2}})]/\epsilon^{\frac{1}{2}},\ s\gtrless 0,$$

and the meridional velocities are

$$v(\eta)=i\eta\exp(-\eta^2/2). \quad (3.8)$$

The asymptotic behavior of the eigensolutions as $\epsilon \to +\infty$ can be described by an ad hoc equatorial β-plane approximation. This simplified geometry has been applied with success in the studies of Matsuno (1966) and Lindzen (1967). The Kelvin wave has meridional velocity identically equal to zero in this simplified geometry.

3) ASYMPTOTIC SOLUTIONS AS $\epsilon \to -\infty$

The solutions as $\epsilon \to =-\infty$ are asymptotically described in terms of generalized Laguerre polynomials. The energy of the motions is concentrated around the North and South Poles and is small near the equator. This fact implies that the motions are hemispherically independent and explains the pairing of eigenvalues of symmetric and antisymmetric solutions evident on Figs. 4 and 5. (We corrected several misprints on pp. 553–556 of Longuet-Higgins.)

Type 4: The motions of type 4 take place in inertial circles moving westward. The frequencies are

$$\lambda=1+(s-2\nu)/(-\epsilon)^{\frac{1}{2}},\quad \nu=0, 1, 2, \ldots; s<0,$$

and the meridional velocities

$$v(\omega)=-i(-\epsilon)^{\frac{1}{4}}\exp(-\omega^2/2)\omega^{|s|-1}L_\nu^{(|s|-1)}(\omega^2),$$
$$\omega=(-\epsilon)^{\frac{1}{4}}\theta. \quad (3.9)$$

Here $L_\nu^s(x)$ is the generalized Laguerre polynomial of degree ν and order s [Jeffreys and Jeffreys (1972), p. 616].

Type 5: This type of motion is in inertial circles and propagate eastward for $s>0$. The frequencies are

$$\lambda=1-\{s+2\nu+2\}/(-\epsilon)^{\frac{1}{2}},$$
$$\nu=0, 1, 2, \ldots \quad \text{and} \quad s=0, 1, 2, \ldots,$$

and the meridional velocities

$$v(\omega)=-i(-\epsilon)^{\frac{1}{4}}\exp(-\omega^2/2)\omega^{s+1}L_\nu^{(s+1)}(\omega^2). \quad (3.10)$$

The motions of type 4 and 5 have kinetic energy much larger than the total potential energy.

Type 6: This type of motion consists of waves propagating slowly eastward. The energy is mostly potential energy, concentrated around the poles $(\mu=\pm 1)$. This type of motion is a linearized form of the motion analyzed by Burger (1958) under the scaling assumptions of negligible acceleration and very large horizontal scale. Phillips (1963) in his discussion of "geostrophic motion of type 2," anticipated that if Burger's motion did exist in the atmosphere, it must be forced. This is consistent with the negative values of ϵ for type 6. The eigenfrequencies and the eigenfunctions are

$$\left.\begin{aligned}\lambda&=s\{1+[2(s+2\nu+1)]/(-\epsilon)^{\frac{1}{2}}\}/(-\epsilon),\\ &\qquad \nu=0, 1, 2, \cdots, s\gtrless 1\\ v&=-i(-\epsilon)^{\frac{1}{4}}\exp(-\omega^2/2)\omega^{s-1}L_\nu^{(s)}(\omega^2)\end{aligned}\right\}. \quad (3.11)$$

4) ASYMPTOTIC SOLUTIONS FOR $s=0$ AND $\lambda \to 0$

The numerical calculations by Longuet-Higgins (1968) also suggested an asymptotic behavior for $s=0$ and very small frequencies ($\lambda \to 0$). The asymptotic solutions appear as an eigenvalue problem for ϵ, the values of which are found to be finite, negative numbers. This asymptotic behavior is classified as type 7 by Longuet-Higgins.

d. Relevance of the solutions

Theory and applications of atmospheric tides have been discussed thoroughly in Chapman and Lindzen (1970). Among the various forced tides let us show how the "negative equivalent depths" appear in the context of Fig. 1. The solar semi-diurnal thermal tide, for example, needs only the positive ϵ eigensolutions for the forcing to be expanded (the line $s=-2$ and $\lambda=1$ only intercepts surfaces of positive ϵ in Fig. 1). On the other hand, the solar diurnal thermal tide does need both the positive and the negative ϵ eigensolutions (the line $s=-1$ and $\lambda=0.5$ intercepts both surfaces of positive and of negative ϵ in Fig. 1). The importance of the negative ϵ eigensolutions for this problem was first recognized by Lindzen (1966).

Tidal theory has also been applied with success in the analysis of stratospheric equatorial motions. Yanai and Maruyama (1966) have found observational evidence of stratospheric wave disturbances over the tropical Pacific with $s\approx -4$ and $\lambda\approx 0.1$–0.125, being identified as a mixed Rossby-gravity mode (Maruyama, 1967). Wallace and Kousky (1968) have observed and identified the Kelvin wave with $\lambda\approx 0.03$–0.05 with suggested small s. Tropospheric wave analyses have also been made by Wallace (1971), where a review of tropical wave studies is also presented.

4. Balance equations: Eigenvalues and asymptotic relations

Our attention is again focused upon Eqs. (3.2)–(3.4) but with $\alpha'=\alpha=0$. These determine the latitudinal dependence of the linearized balance equations. (Making $\alpha'=0$ changes a prognostic equation into a diagnostic equation: the equation of balance.)

The eigenvalues and eigenfunctions of these equations are to be compared with those of the LTE summarized in Section 3. The possible asymptotic solutions to the equations will also be studied.

a. Integral theorem for the balance equations

In a way analogous to the method used to form an energy equation, one gets an explicit equation for the frequency by multiplying (3.2) by P^*, (3.3) by Q^* ($\alpha'=0$), and (3.4) by R^* (the asterisks mean complex conjugate). The three equations are then added and the resulting expression is written in flux form as

$$\begin{aligned}\lambda[s^2(1-\mu^2)^{-1}PP^*+(1-\mu^2)(dP/d\mu)(dP^*/d\mu)+\epsilon RR^*] \\ =-sPP^*+\alpha(sQQ^*)+(d/d\mu) \\ \times[(1-\mu^2)(\lambda P^*dP/d\mu+\mu QdP^*/d\mu-\mu P^*dQ/d\mu \\ +R^*dQ/d\mu-QdR^*/d\mu)]. \quad (4.1)\end{aligned}$$

Integrating (4.1) from $\mu=-1$ to $\mu=+1$, with the flux terms vanishing at both poles, we get the following integral theorem:

$$\lambda=[-sI_1+\alpha(sI_5)]/[s^2I_2+I_3+\epsilon I_4], \quad (4.2)$$

where

$$\left.\begin{aligned} I_1&=\int_{-1}^{1}|P|^2d\mu, \quad I_2=\int_{-1}^{1}(1-\mu^2)^{-1}\left|\frac{dP}{d\mu}\right|^2d\mu, \\ I_3&=\int_{-1}^{1}(1-\mu^2)\left|\frac{dP}{d\mu}\right|^2d\mu, \quad I_4=\int_{-1}^{1}|R|^2d\mu, \\ I_5&=\int_{-1}^{1}|Q|^2d\mu \end{aligned}\right\}. \quad (4.3)$$

The spectrum of possible frequencies is represented by (4.2), where λ is expressed by means of positive integrals of the eigenfunctions, the wavenumber s, and the parameter ϵ.

An important result from (4.2) is that for the balance equations ($\alpha=0$) only westward propagating modes are solutions when ϵ is positive. (This powerful constraint is no longer true if $\alpha=1$.) For $s=0$ the only solutions are $\lambda=0$, except for some finite negative values of ϵ for which the denominator of (4.2) vanishes. These values of ϵ are discussed in Section 4b and correspond to the asymptotic type 7 (Section 3). From this behavior of the eigenvalues for $s=0$ we may infer that if the balance equations are to have part of the mixed Rossby-gravity mode as a solution, it cannot "cross" the $s=0$ axis (see Fig. 2).

It might be pointed out that the denominator of (4.2) is essentially the sum of solenoidal kinetic plus total potential energy, whereas the numerator comes from the variability of the Coriolis parameter in Eqs. (2.7) and (2.8).

In our numerical study of the eigensolutions we have also derived an equivalent integral theorem for a truncated matrix (Moura, 1974).

b. The eigenvalues of the balance equations

1) METHOD OF SOLUTION

Solutions of (3.2)–(3.4) are obtained in the conventional manner by expanding $P(\mu)$ and $Q(\mu)$ in surface

spherical harmonics $P_n^s(\mu)$ [Korn and Korn (1968), p. 870], and then solving a system of algebraic equations for the coefficients:

$$\left.\begin{aligned} P&=\sum_{n=s}^{\infty} B_n^s P_n^s(\mu)\\ Q&=\sum_{n=s}^{\infty} A_n^s P_n^s(\mu)\end{aligned}\right\}. \tag{4.4}$$

Making use of the properties of $P_n^s(\mu)$ we get

$$R(\mu)=-1/(\lambda\epsilon)\sum_{n=s}^{\infty} n(n+1)A_n^s P_n^s(\mu), \tag{4.5}$$

and the following recurrence relations for A_n^s and B_n^s:

$$[\lambda n(n+1)+s]B_n^s-[n(n+2)(n+s+1)/(2n+3)]A_{n+1}^s -[(n-1)(n+1)(n-s)/(2n-1)]A_{n-1}^s=0, \tag{4.6}$$

$$[n^2(n+1)^2/(\lambda\epsilon)-\alpha s]A_n^s +[n(n+2)(n+s+1)/(2n+3)]B_{n+1}^s +[(n-1)(n+1)(n-s)/(2n-1)]B_{n-1}^s=0. \tag{4.7}$$

Eq. (4.7) (with $\alpha=0$) is solved for A_n^s and the result used in (4.6) to give (see Appendix B where the α term is kept)

$$d_{n-2}B_{n-2}^s+(a_n+b_n-\lambda)B_n^s+c_{n+2}B_{n+2}^s=0, \tag{4.8}$$

where

$$\left.\begin{aligned} a_n&=-\lambda\epsilon\{n(n-s+1)(n+s+1)/ [(n+1)^3(2n+1)(2n+3)]+(n+1)(n-s) \times(n+s)/[n^3(2n-1)(2n+1)]\},\\ &\quad \text{for } s=0,\ n=1,2,3,\ldots,\quad a_1=-\lambda\epsilon/30\\ b_n&=-s/[n(n+1)],\quad \text{for } s=0,\ b_n=0,\\ c_n&=-\lambda\epsilon\{(n+1)(n+s-1)(n+s)/ [(n-1)^2n(2n-1)(2n+1)]\}\\ d_n&=-\lambda\epsilon\{n(n-s+1)(n-s+2)/ [(n+1)(n+2)^2(2n+1)(2n+3)]\}\end{aligned}\right\}. \tag{4.9}$$

There are two separate types of motions described by the algebraic system (4.8). One for which $(n-s)$ is even will be denoted as *antisymmetric modes* (v and P are even functions of μ; u, Q, R are odd functions of μ) and another for which $(n-s)$ is odd will be denoted *symmetric modes* (v and P are odd functions; u, Q, R are even functions of μ).

In order to solve the homogeneous systems (4.8) we will fix values of the product $\lambda\epsilon$ and treat the consequent ordinary eigenvalue problem for λ. There is an infinite number of eigenvalues from which we are interested only in the lowest modes. The procedure is to truncate the tridiagonal matrices taking only the first $N\times N$ elements. The value of N is dictated by the convergence of the eigenvalues being sought and an energetically consistent way to truncate the matrices is used (Moura, 1974).

2) Discussion of the computed eigenvalues

Fig. 6 is the counterpart of Fig. 1 for the balance equations, showing the surfaces $n=n(\lambda,s,\epsilon)$.

For positive values of ϵ only westward propagating modes ($s<0$) are solutions. The eigenvalue λ is confined to the range $(0,\frac{1}{2})$ and the westward gravity waves are absent. Referring for further details to Fig. 9 (for $s=-1$), we note the following facts about the remaining (Rossby) modes. First, there is excellent agreement with the LTE solutions for small positive values of ϵ (waves of the second class). As ϵ is increased the highest frequency mode begins to have a somewhat higher frequency than the mixed Rossby-gravity mode of the tidal equations. The lower frequency modes have good agreement for the antisymmetric modes, but the symmetric modes begin to assume the frequency appropriate to the neighboring antisymmetric mode.

For negative values of ϵ there are eastward and westward propagating solutions, but λ has the range $(0,\infty)$ instead of the range $(0,1)$ of the LTE. The westward modes (Fig. 9) are an analytical continuation of the modes of second class for small negative ϵ, but instead of showing an accumulation at $\lambda=1$ (Section 3, type 4) as $(-\epsilon)$ is increased, symmetric and antisymmetric modes "cross" and become independent of λ at finite negative values of ϵ.

For $s=0$ and $\epsilon<0$, the allowable values of ϵ are independent of λ (see Fig. 7). This independence of λ appears in the system (4.8), where $s=0$ makes b_n vanish, allowing λ to be divided out of each row in the matrix. The ϵ values are numerically identical with the values given by Longuet-Higgins for the asymptotic type 7 ($\epsilon<0$, $s=0$, $\lambda\to 0$). For $\epsilon<0$ and $s>0$ (eastward propagation) we have recovered (Fig. 8) the limiting low-frequency "Burger" solutions corresponding to the type 6 of Longuet-Higgins (Section 3). As the frequency is increased, however, the pairing described in Section 3 for type 6 does not occur. Instead, both symmetric and antisymmetric modes at large λ have eigenvalues $(-\epsilon)$ independent of λ.

We now parallel Longuet-Higgins' approach by examining the asymptotic behavior suggested by the numerical results.

3) Asymptotic solutions as $\epsilon\to 0$

These asymptotic solutions are obtained directly from the system (4.8) as $\lambda\epsilon\to 0$. The square matrices become diagonally dominant ($c_n, d_n\to 0$) and the eigenvalues become those for the "second class"

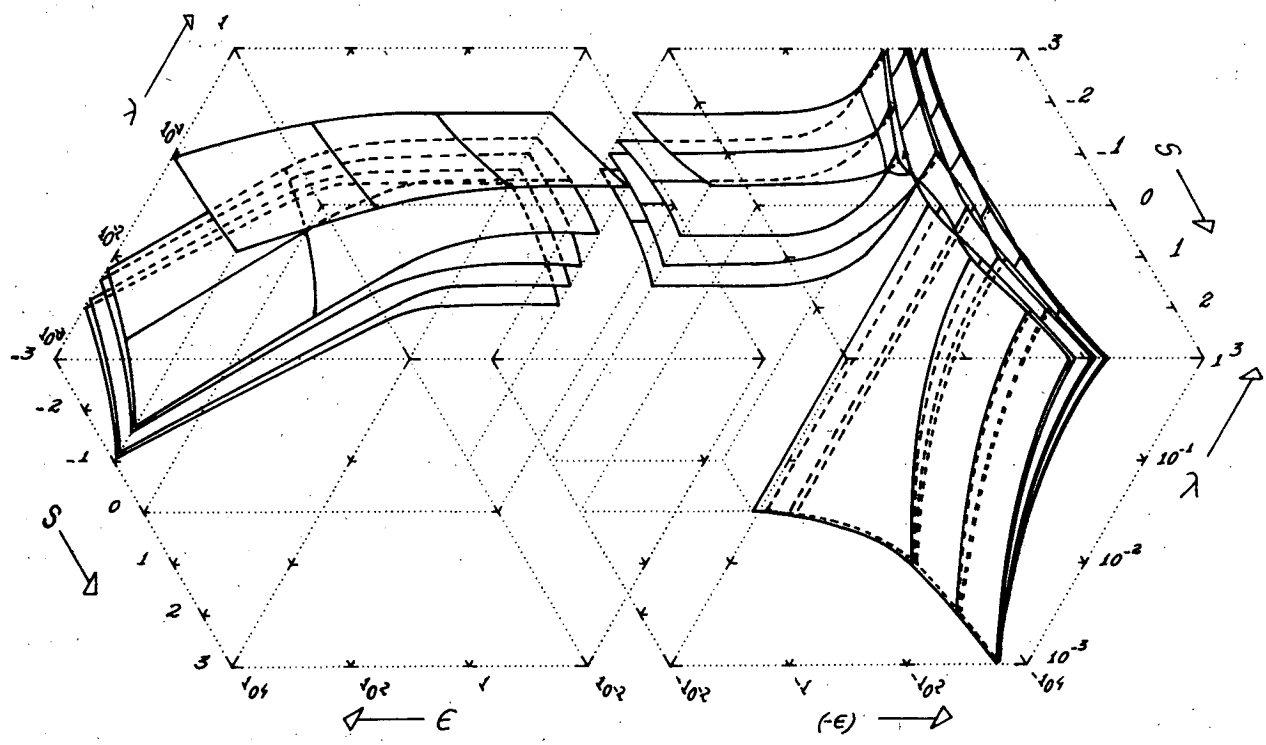

FIG. 6. Eigenvalues for the balance equations. Surfaces are shown for selected latitudinal modes (see legend to Fig. 1). The surfaces for negative ϵ continue upward above $\lambda=1$ instead of accumulating at $\lambda=1$ as they do in Fig. 1.

Rossby waves:

$$\lambda=\frac{-s}{n(n+1)+\epsilon\left[\dfrac{(n+1)^2(n-s)(n+s)}{n^2(2n-1)(2n+1)}+\dfrac{n^2(n-s+1)(n+s+1)}{(n+1)^2(2n+1)(2n+3)}\right]}, \quad s<0. \tag{4.10}$$

(The term multiplied by ϵ in the denominator comes from the first-order terms in the expansion in powers of small ϵ.)

The waves of the first class (gravity waves) do not appear as solutions in this limiting value of ϵ. In this sense the gravity waves are "filtered out" by the use of the balance system. Fig. 9 shows this asymptote for the case $s=-1$.

4) ASYMPTOTIC SOLUTIONS AS $\epsilon\to-\infty$

There exist solutions with small frequencies as $\epsilon\to-\infty$ (Fig. 8). They are obtained from an expansion in power series of $(-\epsilon)^{-\frac{1}{2}}$ as follows:

$$\lambda=s(-\epsilon)^{-1}[\lambda_0+(-\epsilon)^{-\frac{1}{2}}\lambda_1+\cdots],$$
$$P=[P_0+(-\epsilon)^{-\frac{1}{2}}P_1+\cdots],$$
$$Q=(-\epsilon)^{-\frac{1}{2}}[Q_0+(-\epsilon)^{-\frac{1}{2}}Q_1+\cdots],$$
$$R=[R_0+(-\epsilon)^{-\frac{1}{2}}R_1+\cdots].$$

Since the solutions are expected to be confined to the vicinity of the poles, we use the stretched coordinate $\omega=(-\epsilon)^{\frac{1}{2}}\theta$ [or $\omega=(-\epsilon)^{\frac{1}{2}}(\pi-\theta)$ for the South Pole]. In order to find the solutions it is necessary to go up to first order in the expanding parameter. The zeroth order corresponds to a β-plane approximation, which geometry we know to be incapable of describing these motions (see Phillips, 1963, p. 161). It is then expected that the solutions emanate from additional constraints in higher order terms in $(-\epsilon)^{-\frac{1}{2}}$. The eigensolutions are, asymptotically (Moura, 1974):

$$\lambda=s[1+2(s+2\nu+1)/(-\epsilon)^{\frac{1}{2}}]/(-\epsilon), \qquad \nu=0,1,2,\ldots,\ s>0, \tag{4.11}$$

$$\left.\begin{aligned} P=R&=\exp(-\omega^2/2)\omega^s L_\nu^{(s)}(\omega^2)\\ [\omega^2(d^2/d\omega^2)+\omega(d/d\omega)-s^2]Q&=-s(-\epsilon)^{-\frac{1}{2}}\omega^2 P\end{aligned}\right\}. \tag{4.12}$$

The solutions correspond to Longuet-Higgins' type 6 as discussed in Section 3.

It was pointed out earlier that this type of wave follows from the scale analysis of Burger (1958). His scale analysis assumed that the divergence and vorticity were of equal magnitude, so that the vorticity equation reduces to

$$f\nabla\cdot\mathbf{V}=-\beta v, \text{ or } \nabla\cdot\mathbf{V}=-\tan\theta(v/a)=\nabla\cdot\mathbf{V}_{\text{geo}}. \tag{4.13}$$

The balance equations on the other hand are derived (from the point of view of accuracy) by assuming that the vorticity (or streamfunction) is greater than the divergence (or velocity potential), and (4.12) verifies that this is indeed true for these motions. The apparent paradox with (4.13) is solved by noting that the solutions are concentrated near the pole, where $\tan\theta$ is small and the geostrophic wind is essentially nondivergent.

5) ASYMPTOTIC SOLUTIONS AS $\epsilon \to +\infty$

Our attempts to describe this asymptotic behavior analytically have not been completely successful. In order to study this case we use the stretched coordinate $u=\epsilon^{\frac{1}{4}}\mu$ (i.e., the solutions are expected to be concentrated about the equator), and the expanding parameter $\epsilon^{-\frac{1}{4}}$. The following expansion is made:

$$\left.\begin{aligned} \lambda &= \epsilon^{-\frac{1}{2}}(\lambda_0+\epsilon^{-\frac{1}{4}}\lambda_1+\cdots) \\ P &= (P_0+\epsilon^{-\frac{1}{4}}P_1+\cdots) \\ Q &= \epsilon^{-\frac{1}{4}}(Q_0+\epsilon^{-\frac{1}{4}}Q_1+\cdots) \\ R &= \epsilon^{-\frac{1}{4}}(R_0+\epsilon^{-\frac{1}{4}}R_1+\cdots) \end{aligned}\right\}. \tag{4.14}$$

Using (4.14) into (3.2)–(3.4) we arrive at the zeroth order equations (Moura, 1974):

$$\lambda_0 U_0+\eta V_0 = sR_0+sA\eta+C, \tag{4.15}$$

$$-\eta U_0 = (dR_0/d\eta)+A, \tag{4.16}$$

$$sU_0-(dV_0/d\eta)=\lambda_0 R_0. \tag{4.17}$$

In these equations $U_0=(-dP_0/d\eta)$ and $V_0=(dQ_0/d\eta)+sP_0$ play the role of zonal and meridional velocities. A and C are integration constants: $A=-(dR_0/d\eta)_{\eta=0}$; $C=(\lambda_0U_0-sR_0)_{\eta=0}$. Note that if they were zero, (4.15)–(4.17) would correspond directly to the original equations of motion with $(\partial v/\partial t)=0$.

The following equation for V_0 is obtained from (4.15)–(4.17), when $\lambda_0^2 \neq s^2$:

$$\{(d^2/d\eta^2)-(s/\lambda_0)-\eta^2\}V_0 = A(s\eta^2-\lambda_0)-C\eta. \tag{4.18}$$

If $A=C=0$, (4.18) leads immediately to Longuet-Higgins' solutions of type 2 (Section 3).

However, we know from the accurate matrix solutions shown on Fig. 9 that the *symmetric* modes of the balance equations differ from this at large ϵ. Let us write (4.18) separately for symmetric ($V_0^{(s)}$) and for antisymmetric modes ($V_0^{(a)}$).

Symmetric modes (R_0, U_0, Q_0 even; V_0, P_0 odd)

$$[(d^2/d\eta^2)-(s/\lambda_0)-\eta^2]V_0^{(s)} = -C\eta. \tag{4.19}$$

Antisymmetric modes (R_0, U_0, Q_0 odd; V_0, P_0 even)

$$[(d^2/d\eta^2)-(s/\lambda_0)-\eta^2]V_0^{(a)} = -A(s\eta^2+\lambda_0). \tag{4.20}$$

The boundary conditions on V_0 are that $V_0 \to 0$ as $|\eta| \to \infty$ [i.e., V_0 must decay rapidly away from the equator for the β-plane (zeroth-order) to be a valid approximation]. The homogeneous solutions of the parabolic cylinder equation (4.18) obeying these boundary conditions are the Hermite functions $\exp(-\eta^2/2)H_\nu(\eta)$ with the imposed eigenvalue condition $-s/\lambda_0=2\nu+1$, where ν is equal to a positive integer.

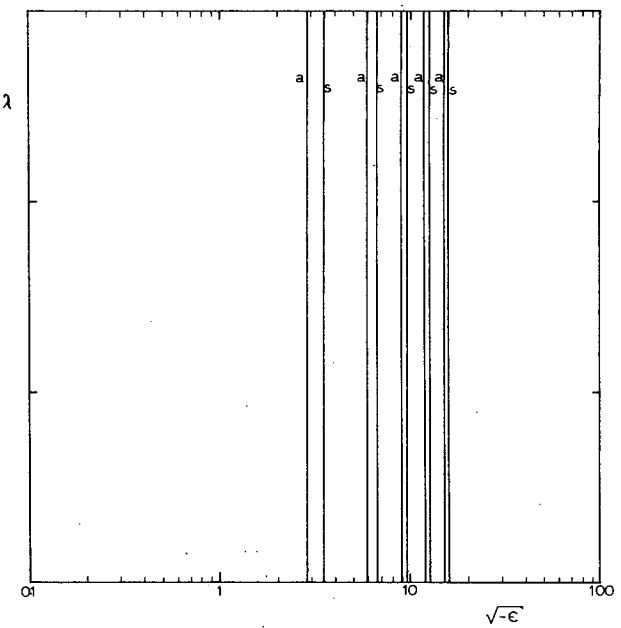

FIG. 7. Eigenvalues for the balance equations for the longitudinal wavenumber $s=0$. They correspond to the asymptotic type 7 ($\epsilon<0$, $\lambda \to 0$) described by Longuet-Higgins (compare with Fig. 3). The eigenvalues (ϵ) are independent of the frequency (λ). The letters a and s stand for modes with geopotential antisymmetric and symmetric about the equator.

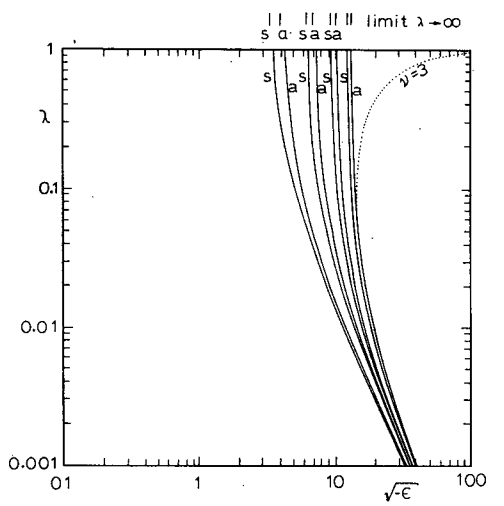

FIG. 8. Eigenvalues for the balance equations for $s=1$. The limiting solutions for small frequencies agree with Longuet-Higgins' type 6 (compare with Fig. 4). However, for high frequencies, the modal curves continue upward above $\lambda=1$ and become independent of λ, with the limiting solutions ($\lambda \to \infty$) indicated. (These modes are here called "Burger" modes.)

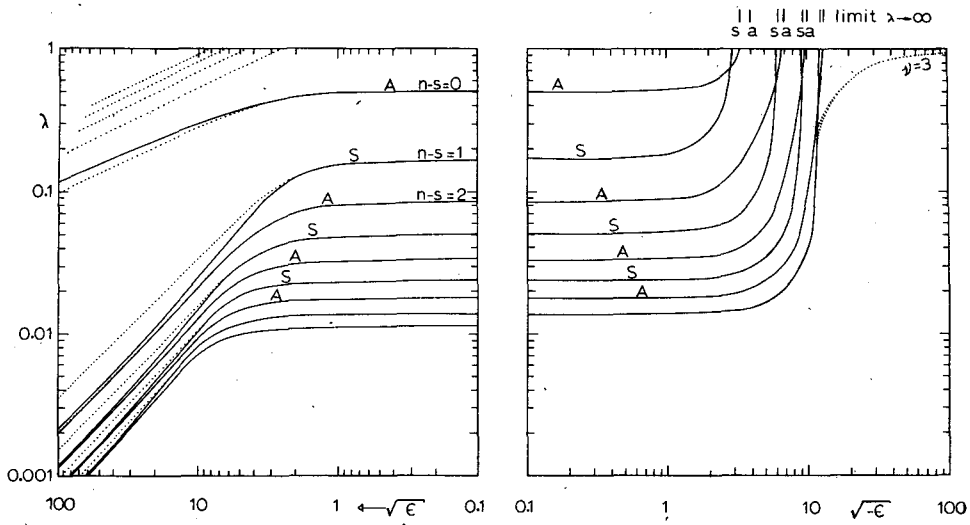

FIG. 9. Eigenvalues for the balance equations for $s=-1$. The frequencies are in the range $(0, \frac{1}{2})$ for positive values of ϵ. The curves for negative values of ϵ have symmetric (S) and antisymmetric (A) modes crossing and continue upward above $\lambda=1$, with the limiting solutions ($\lambda \to \infty$) indicated (compare with Fig. 5). The dotted curves correspond to some of the engenvalues for the Laplace's tidal equations.

Our matrix computations have revealed that the eigensolutions for the antisymmetric modes are described well by (4.20) with $A=-(dR_0/d\eta)_{\eta=0}=0$. This implies that although R_0 is an odd function of η, it has a zero slope at $\eta=0$ (as in fact happens for the type 2 solutions of the LTE). That, in turn, tells us that the zonal motions are geostrophically balanced in the equatorial region for both kind of symmetries [clearly seen from (4.16)].

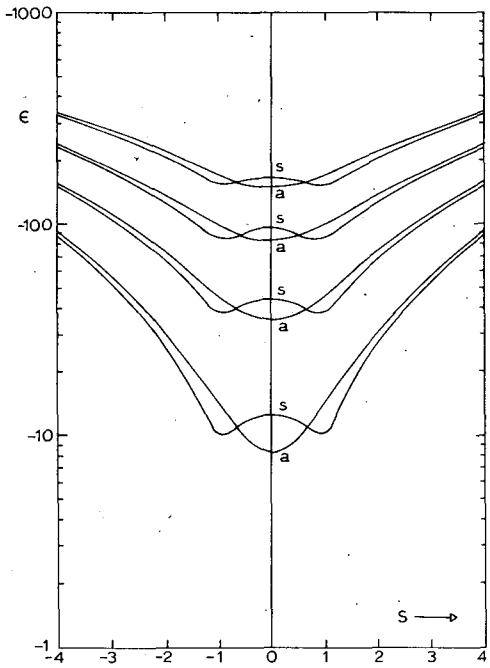

FIG. 10. Eigenvalues for the balance equations for $\lambda=10$. These solutions appear for negative values of ϵ only. The curves show crossing of symmetric and antisymmetric modes.

On the other hand, the (matrix) computed eigensolutions for the symmetric modes show quite different results. They evidently cannot be described by Eq. (4.19) with $C=0$, contrary to what happens for LTE (type 2 solutions with $\nu=1, 3, 5, \ldots$). The eigenvalues show noticeable discrepancy when contrasted to those of LTE, as shown in Fig. 9. The matrix computed eigenfunctions for the meridional velocity (discussed in Section 5) show that at large positive ϵ the antisymmetric modes are confined to low latitudes, agreeing well with the tidal solutions, but the meridional velocity for the symmetric modes has an appreciably larger amplitude in high latitudes than do the tidal solutions. The equatorial expansion in η evidently breaks down to some extent for these solutions.

In Section 7 it will be shown that these symmetric modes, when calculated for the modified balance system ($\alpha=1$), agree much better with Longuet-Higgins' results.

6) BEHAVIOR OF THE SOLUTIONS FOR $s=0$

The eigenvalues for $s=0$ are independent of frequency. They correspond to finite negative values of ϵ which agree with those of type 7 ($\lambda \to 0$; Section 3) and are such that the denominator of (4.2) vanishes (i.e., $I_3=-\epsilon I_4$). The same results are found if $\alpha=1$, since s also multiplies this term in (4.2). Let us call $u_*=(1-\mu^2)(dP/d\mu)$ and $\lambda v_*=(1-\mu^2)(dQ/d\mu)$ and write Eqs. (3.1)–(3.4) with $s=0$ ($\alpha'=0$):

$$-\lambda(du_*/d\mu)+\lambda(d\mu v_*/d\mu)=0, \tag{4.21}$$

$$(d\mu u_*/d\mu)=(d/d\mu)(1-\mu^2)(dR/d\mu), \tag{4.22}$$

$$\lambda(dv_*/d\mu)=\lambda\epsilon R. \tag{4.23}$$

These equations are now independent of λ [for $\lambda=0$

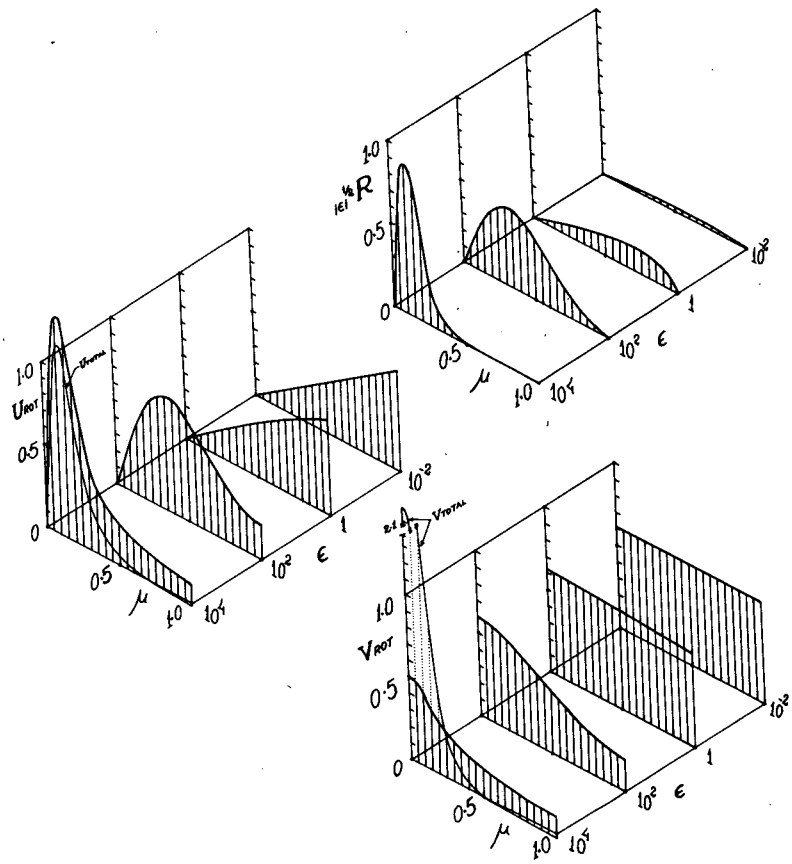

FIG. 11. Eigenfunctions for the balance equations for the "mixed Rossby-gravity" ($\epsilon>0$) mode ($n-s=0$), with $s=-1$, showing the latitudinal distributions of the geopotential (R) and the rotational parts of the zonal ($U_{\rm rot}$) and meridional ($V_{\rm rot}$) velocities. The solutions become more confined to low latitudes as ϵ is increased. At large values of ϵ, the divergent part of the meridional velocity becomes larger than the rotational part for this mode.

the solution is $v_*=0$ and zonal geostrophy $\mu u_* = (1-\mu^2)(dR/d\mu)]$ and are manipulated to give

$$(1-\mu^2)(d^2v_*/d\mu^2)-\epsilon\mu^2 v_*=0. \qquad (4.24)$$

This eigenvalue problem (ϵ is the eigenvalue with $v_*=0$ at $\mu=\pm1$) is the same as that for Longuet-Higgins' type 7. It also appears in a work of Leovy[2] (1964), where (4.24) is solved by a series of Gegenbaur polynomials. The values of ϵ are shown in Fig. 7.

7) ASYMPTOTIC BEHAVIOR AS $\lambda\to\infty$

There are no free solutions (positive ϵ) with frequencies greater than $\lambda=\frac{1}{2}$; high-frequency response of the balance equations occurs only in the case of forcing (negative ϵ).

Our numerical computations of the eigenvalues have revealed the existence of high-frequency solutions for both westward and eastward propagating waves. In addition, the eigenvalues tend to become independent of λ for finite negative value of ϵ. The resulting equations are unfortunately as complicated to solve as the system (3.2)–(3.4). The limiting eigenvalues are shown in Figs. 7–9 and are summarized in Fig. 10.

[2] Pointed out to the author by one of the reviewers.

5. Eigenfunctions

The eigenfunctions of the linearized balance equations are presented graphically in this section. The normalization factor used makes the total energy (rotational kinetic plus potential) integrated over the globe equal to $\pi/2$. This in turn ensures that

$$s^2I_2+I_3+|\epsilon|I_4=1,$$

where I_2, I_3, I_4 are the integrals defined in Section 4 and the absolute value of ϵ is taken for $\epsilon<0$ modes. This normalization procedure (discussed in Appendix B) is similar to that used by Longuet-Higgins (1968). We have chosen to present the variables $|\epsilon|^{\frac{1}{4}}R$, representing the latitudinal dependence of the geopotential, $U_{\rm rot}=-(1-\mu^2)^{\frac{1}{2}}(dP/d\mu)$ corresponding to the latitudinal dependence of the rotational part of the zonal velocity, and $V_{\rm rot}=s(1-\mu^2)^{-\frac{1}{2}}P$ corresponding to the latitudinal dependence of the rotational part of the meridional velocity. The formulas used for these are

those at the end of Appendix B with 50 elements in each expansion and evaluation of the series made at an evenly distributed set of 41 points between $\mu=0$ and $\mu=1$. [To numerically check the eigenfunctions and eigenvalues obtained from the series, we have also introduced these values into a second-order, finite-difference analog of (3.2)–(3.4). The resulting finite-difference equations were typically in error of order $(1/40)^2$.]

The results are shown in Figs. 11–19. Only the first three modes are presented for $s=1$ and $s=-1$. The changes in the modal structure are shown as a function of the parameter ϵ. The eigenfunctions have significant amplitude at all latitude, for small positive or negative values of ϵ. However, as $|\epsilon|$ is increased, the solutions get trapped to some extent in equatorial or polar latitudes, depending on the sign of ϵ.

At low frequencies, the rotational part of the zonal and meridional velocities generally accounts for most of the zonal and meridional velocites. One exception appears for the mixed mode (see Fig. 11) as ϵ is increased. In this case the total U and V velocities are confined more to low latitudes. At high frequencies (which occur only with negative values of ϵ), the divergent part of U and V dominate over the rotational parts. These eigenfunctions are, of course, unrealistic in light of the balance approximation assumption that divergence$\ll$vorticity. Fortunately these modes would only appear if high-frequency forcings are imposed upon the system.

Fig. 20 illustrates our discussion concerning the symmetric and antisymmetric modes of the asymptotic expansion $\epsilon \to +\infty$ (Section 4). The total meridional velocities of the first and second "equatorial Rossby" modes (symmetric and antisymmetric, respectively) for $s=-1$ are plotted in contrast with the asymptotic solutions of type 2 (Section 3). It is apparent that the first symmetric mode [as computed using the system (4.8)] cannot be described by (3.7) with $\nu=1$ due to the large disagreement. It has as extra zero crossing between $\mu=0$ and $\mu=1$ and significant amplitude even at high latitudes. On the other hand, the antisymmetric mode agrees very well with the corresponding asymptotic solution, except for a small discrepancy at extra-equatorial latitudes. It can be fairly well described by (3.7) with $\nu=2$.

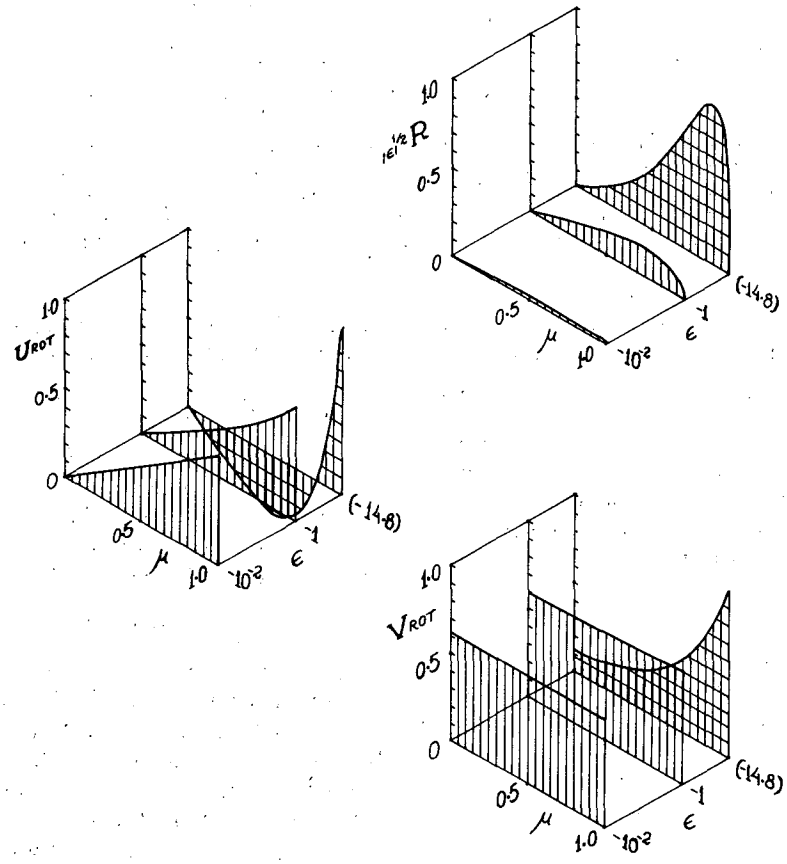

FIG. 12. As in Fig. 11 for the continuation ($\epsilon<0$) of the "mixed Rossby-gravity" mode. The cross-hatched eigenfunctions correspond to the limiting $\lambda \to \infty$ ($\epsilon<0$) solutions.

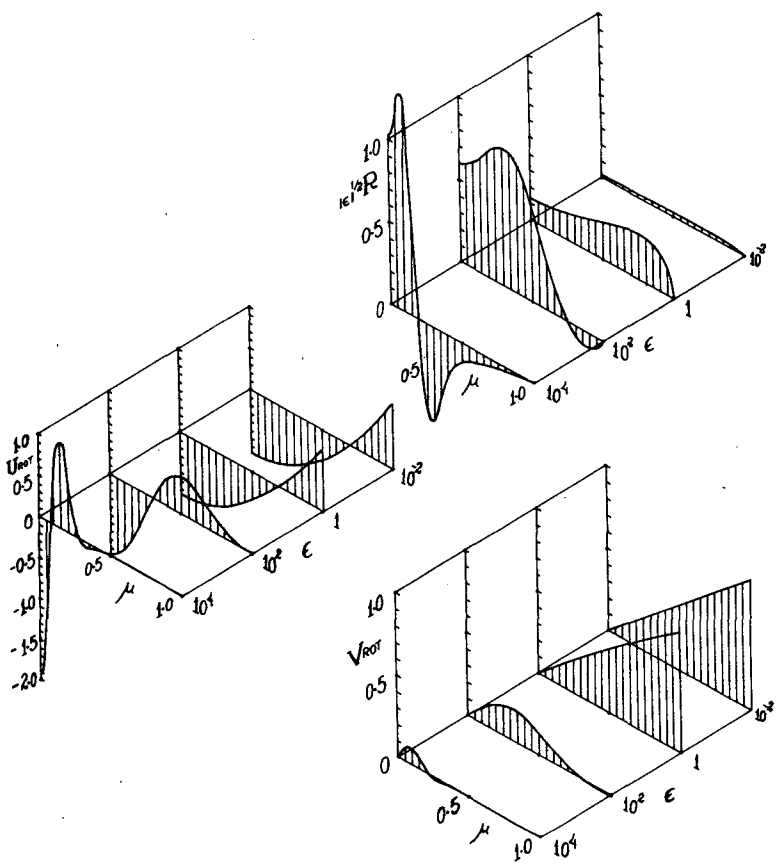

FIG. 13. Eigenfunctions for the balance equations for the $(n-s)=1$ Rossby mode, with $s=-1$. The latitudinal structure of the geopotential (R) and the rotational parts of the zonal ($U_{\rm rot}$) and meridional ($V_{\rm rot}$) velocities are shown for several positive values of ϵ. This mode, at large ϵ, differs from Laplace's tidal solutions of type 2 for $\nu=1$.

6. Stability study of a basic zonal velocity profile

In the previous sections we have studied the latitudinal structure of the solutions of the balance equations on a resting basic state. We have shown that all possible frequencies are real [integral theorem (4.2)].

The inclusion of a basic zonal flow in Eqs. (2.7)–(2.11) may allow for complex values among the possible frequencies. Some of the modal solutions will then be damped while others will grow exponentially with time. The perturbation solutions with a positive growth rate (imaginary part of the frequency>0) are said to be barotropically or baroclinically unstable (or both), depending on their energy sources.

We will focus our attention on the baroclinic instability problem with a simple family of zonal wind profiles $\bar{U}=a\alpha(p)(1-\mu^2)^{\frac{1}{2}}(1+\delta\mu^2)$. The use of this basic zonal velocity in the continuous equations (2.7)–(2.11), however, makes the separation of vertical and horizontal structures impossible. In order to handle this difficulty we will make use of a simple two-layer model, which is still able to provide the conversion of available potential energy to feed the growing perturbations.

a. The model equations

The basic state under study satisfies the relations

$$\nabla\bar{\psi}=-\hat{\jmath}a\alpha(p)(1-\mu^2)^{\frac{1}{2}}(1+\delta\mu^2), \tag{6.1}$$

$$\nabla\bar{\Phi}=-\hat{\jmath}a\alpha(p)\mu(1-\mu^2)^{\frac{1}{2}}(1+\delta\mu^2) \times[2\Omega+\gamma\alpha(p)(1+\delta\mu^2)], \tag{6.2}$$

$$f+\nabla^2\bar{\psi}=2\mu[\Omega+\alpha(p)(1-\delta+2\delta\mu^2)], \tag{6.3}$$

$$\bar{\chi}=\bar{\omega}=0, \tag{6.4}$$

in which $\alpha(p)$ is the functional variation of the basic state zonal velocity with respect to pressure. The index γ, which takes the values 0 or 1, is used in order to compare the two sets of equations (6.5)–(6.8) with and without the γ terms. These γ terms come from the underlined terms in (2.7) and (2.8).

Inserting (6.1)–(6.4) into (2.7)–(2.10) with $\alpha=0$, $\mathbf{F}=0$, $q=0$ and linearizing, we obtain

$$\partial(\mathfrak{L}\psi')/\partial t = -\alpha(p)(1+\delta\mu^2)\partial(\mathfrak{L}\psi')/\partial\phi - 2[\Omega+\alpha(p)(1-\delta+6\delta\mu^2)]\partial\psi'/\partial\phi - 2\mu[\Omega+\gamma\alpha(p)(1-\delta-2\delta\mu^2)]\mathfrak{L}\chi' - 2(1-\mu^2)[\Omega+\gamma\alpha(p)(1-\delta+6\delta\mu^2)]\partial\chi'/\partial\mu + \gamma a^2(d\alpha/dp)(\partial/\partial\mu)[(1-\mu^2)(1+\delta\mu^2)\tilde{\omega}'], \quad (6.5)$$

$$\mathfrak{L}\Phi' = 2\mu[\Omega+\gamma\alpha(p)(1-\delta+2\delta\mu^2)]\mathfrak{L}\psi' + 2(1-\mu^2)[\Omega+\gamma\alpha(p)(1-\delta+6\delta\mu^2)]\partial\psi'/\partial\mu + 2\gamma\alpha(p)\mu(1-\delta+2\delta\mu^2)\mathfrak{L}\psi' - \gamma\alpha(p)(1-\mu^2)(1-\delta\mu^2)\partial(\mathfrak{L}\psi')/\partial\mu + \gamma\alpha(p)\mathfrak{L}[(1-\mu^2)(1+\delta\mu^2)\partial\psi'/\partial\mu], \quad (6.6)$$

$$\partial^2\Phi'/\partial t\partial p = -\alpha(p)(1+\delta\mu^2)\partial^2\Phi'/\partial\phi\partial p + [\Re p_{00}^{-1}(p_{00}/p)^{1-\kappa}d\Theta_s/dp]\tilde{\omega}' + 2(d\alpha/dp)\mu(1+\delta\mu^2)[\Omega+\gamma\alpha(p)(1+\delta\mu^2)]\partial\psi'/\partial\phi, \quad (6.7)$$

$$\mathfrak{L}\chi' = -a^2\partial\tilde{\omega}'/\partial p, \quad (6.8)$$

where $\mathfrak{L}\equiv a^2\nabla^2$ and δ is a parameter. [Note that (6.5)–(6.7) with $\gamma=0$ or $\gamma=1$ reduces to the same set of equations if the basic state is a resting one. Thus, the linearized study presented in previous sections applies to both systems.]

b. *Two-layer model*

The pressure dependence of the perturbation variables will be expressed in finite-difference form by means of a two-layer model, schematically shown in Fig. 21.

Eqs. (6.5), (6.6) and (6.8) are then written for levels 1 and 3 while Eq. (6.7) is written for level 2.

Taking the boundary conditions at $p=p_{00}$ and $p=0$ as $\tilde{\omega}_0'=\tilde{\omega}_4'=0$ (which implies $\chi_1'=-\chi_3'$) and by defining:

$$\left.\begin{aligned} \chi &= \chi_1' = -\chi_3', & \theta &= (\psi_1'-\psi_3')/2 \\ \tau &= (\Phi_1'-\Phi_3')/4\Omega & t' &= 2\Omega t \\ H &= (\Phi_1'+\Phi_3')/4\Omega, & \omega &= (\alpha_1+\alpha_3)/4\Omega \\ \psi &= (\psi_1'+\psi_3')/2, & \Lambda &= (\alpha_1-\alpha_3)/4\Omega \end{aligned}\right\}, \quad (6.9)$$

and assuming

$$\left.\begin{aligned} \tilde{\omega}_3' &= \tilde{\omega}_1' = \tilde{\omega}_2'/2 \\ \psi_2' &= (\psi_1'+\psi_3')/2 \\ \alpha_4-\alpha_2 &= \alpha_2-\alpha_0 = \alpha_3-\alpha_1 = -4\Omega\Lambda \end{aligned}\right\}, \quad (6.10)$$

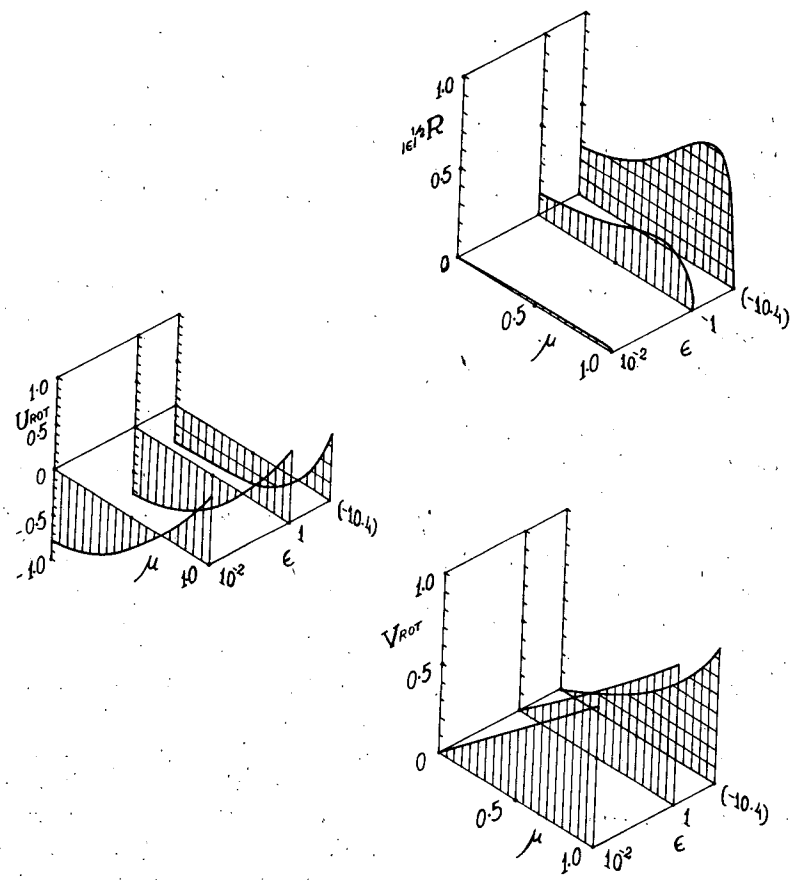

FIG. 14. As in Fig. 13 for the continuation ($\epsilon<0$) of the $(n-s)=1$ Rossby mode. The cross-hatched eigenfunctions correspond to the limiting $\lambda\to\infty$ ($\epsilon<0$) solutions.

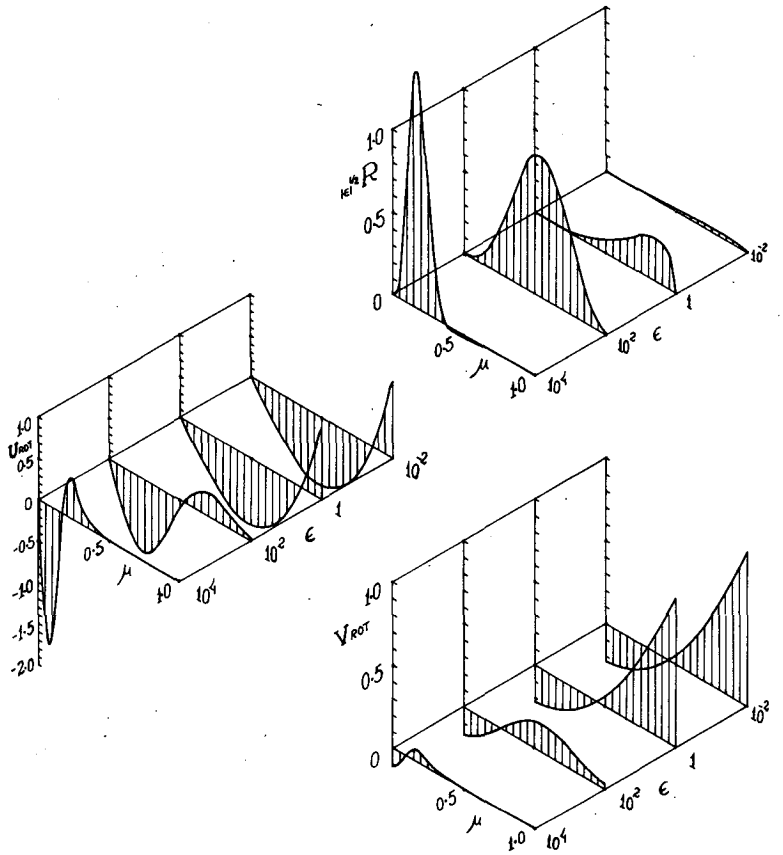

FIG. 15. As in Fig. 13 except for the $(n-s)=2$ Rossby mode. This mode at large ϵ agrees well with the limiting type 2 solutions with $\nu=2$ (Longuet-Higgins).

we arrive at

$$\partial(\mathcal{L}\psi)/\partial t' = -\omega(1+\delta\mu^2)\partial(\mathcal{L}\psi)/\partial\phi - \Lambda(1+\delta\mu^2)\partial(\mathcal{L}\theta)/\partial\phi - [1+2\omega(1-\delta+6\delta\mu^2)]\partial\psi/\partial\phi - 2\Lambda(1-\delta+6\delta\mu^2)\partial\theta/\partial\phi - 2\gamma\Lambda\mu(1-\delta+2\delta\mu^2)\mathcal{L}\chi - 2\gamma\Lambda(1-\mu^2)(1-\delta+6\delta\mu^2)\partial\chi/\partial\mu + \gamma\Lambda(\partial/\partial\mu)[(1-\mu^2)(1+\delta\mu^2)\mathcal{L}\chi], \quad (6.11)$$

$$\partial(\mathcal{L}\theta)/\partial t' = -\omega(1+\delta\mu^2)\partial(\mathcal{L}\theta)/\partial\phi - \Lambda(1+\delta\mu^2)\partial(\mathcal{L}\psi)/\partial\phi - [1+2\omega(1-\delta+6\delta\mu^2)]\partial\theta/\partial\phi - 2\Lambda(1-\delta+6\delta\mu^2)\partial\psi/\partial\phi - \mu[1+2\gamma\omega(1-\delta+2\delta\mu^2)]\mathcal{L}\chi - (1-\mu^2)[1+2\gamma\omega(1-\delta+6\delta\mu^2)]\partial\chi/\partial\mu, \quad (6.12)$$

$$\partial\tau/\partial t' = -\omega(1+\delta\mu^2)\partial\tau/\partial\phi + \Lambda\mu(1+\delta\mu^2)[1+2\gamma\omega(1+\delta\mu^2)]\partial\psi/\partial\phi - S\mathcal{L}\chi, \quad (6.13)$$

$$\mathcal{L}\tau = \mu[1+2\gamma\omega(1-\delta+2\delta\mu^2)]\mathcal{L}\theta + 2\gamma\Lambda\mu(1-\delta+2\delta\mu^2)\mathcal{L}\psi + (1-\mu^2)[1+2\gamma\omega(1-\delta+6\delta\mu^2)]\partial\theta/\partial\mu + 2\gamma\Lambda(1-\mu^2)(1-\delta+6\delta\mu^2)\partial\psi/\partial\mu + 2\gamma\omega\mu(1-\delta+2\delta\mu^2)\mathcal{L}\theta + 2\gamma\Lambda\mu(1-\delta+2\delta\mu^2)\mathcal{L}\psi - \gamma\omega(1-\mu^2)(1+\delta\mu^2)\partial(\mathcal{L}\theta)/\partial\mu - \gamma\Lambda(1-\mu^2)(1+\delta\mu^2)\partial(\mathcal{L}\psi)/\partial\mu + \gamma\omega\mathcal{L}[(1-\mu^2)(1+\delta\mu^2)\partial\theta/\partial\mu] + \gamma\Lambda\mathcal{L}[(1-\mu^2)(1+\delta\mu^2)\partial\psi/\partial\mu], \quad (6.14)$$

$$\mathcal{L}H = \mu[1+2\gamma\omega(1-\delta+2\delta\mu^2)]\mathcal{L}\psi + 2\gamma\Lambda\mu(1-\delta+2\delta\mu^2)\mathcal{L}\theta + (1-\mu^2)[1+2\gamma\omega(1-\delta+6\delta\mu^2)]\partial\psi/\partial\mu + 2\gamma\Lambda(1-\mu^2)(1-\delta+6\delta\mu^2)\partial\theta/\partial\mu + 2\gamma\omega\mu(1-\delta+2\delta\mu^2)\mathcal{L}\psi + 2\gamma\Lambda\mu(1-\delta+2\delta\mu^2)\mathcal{L}\theta - \gamma\omega(1-\mu^2)(1+\delta\mu^2)\partial(\mathcal{L}\psi)/\partial\mu - \gamma\Lambda(1-\mu^2)(1+\delta\mu^2)\partial(\mathcal{L}\theta)/\partial\mu + \gamma\omega\mathcal{L}[(1-\mu^2)(1+\delta\mu^2)\partial\psi/\partial\mu] + \gamma\Lambda\mathcal{L}[(1-\mu^2)(1+\delta\mu^2)\partial\theta/\partial\mu], \quad (6.15)$$

$$\tilde{\omega}_2' = -a^{-2}(\Delta p)\mathcal{L}\chi, \quad (6.16)$$

and $S=(8\Omega^2a^2p_{00})^{-1}\Delta p\mathcal{R}(p_{00}/p_2)^{1-\kappa}(\Theta_{s1}-\Theta_{s3})$ is the nondimensional static stability.

Eqs. (6.11)–(6.14) form a closed system in the variables ψ, θ, τ and χ.

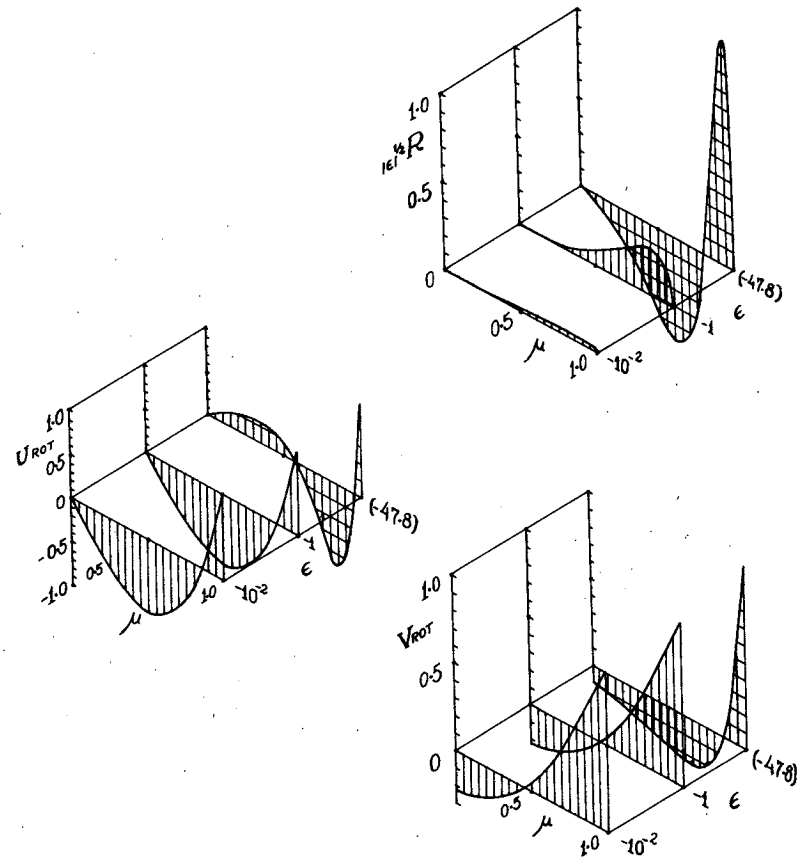

FIG. 16. As in Fig. 14 for the continuation ($\epsilon<0$) of the $(n-s)=2$ Rossby mode.

c. Comparison of the two systems of equations with $\gamma=0$ and $\gamma=1$

We now turn our attention to the comparison of the two systems of equations, (6.11)–(6.14), for $\gamma=0$ and $\gamma=1$. This comparison will be made using only the basic zonal velocity profile $\bar{U}=a\alpha(p)(1-\mu^2)^{\frac{1}{2}}$; i.e., by letting $\delta=0$ in those equations [further study using different profiles is presented in Moura and Stone (1975)]. This profile is able to accentuate the differences between the two sets of equations, since it has large amplitudes in low latitudes, where the behavior of the two sets is most distinct. It corresponds to a state of solid rotation within each layer.

We then seek solutions of the form

$$\begin{bmatrix}\psi\\ \theta\\ \chi\\ \tau\end{bmatrix}=\mathrm{Re}\left\{\sum_{n=s}^{N}\begin{bmatrix}\Psi_n^s(t')\\ \Theta_n^s(t')\\ iX_n^s(t')\\ T_n^s(t')\end{bmatrix}P_n^s(\mu)\exp(is\phi-i\omega st')\right\}, \quad (6.17)$$

where the latitudinal dependence has been truncated in the associated Legendre function expansion for computational purposes.

After using the properties of $P_n^s(\mu)$, Eqs. (6.11)–(6.14) become

$$\dot{\Psi}_n^s=e_n\Psi_n^s+f_n\Theta_n^s+A_nX_{n-1}^s-B_nX_{n+1}^s, \quad (6.18)$$

$$\dot{\Theta}_n^s=e_n\Theta_n^s+f_n\Psi_n^s+C_nX_{n-1}^s+D_nX_{n+1}^s, \quad (6.19)$$

$$T_n^s=Sn(n+1)[-w_n(c_n\Psi_{n-1}^s+d_n\Psi_{n+1}^s)-X_n^s], \quad (6.20)$$

$$T_n^s=Sn(n+1)[w_n(a_n\Theta_{n-1}^s+b_n\Theta_{n+1}^s)+\Gamma_n(a_n\Psi_{n-1}^s+b_n\Psi_{n+1}^s)], \quad (6.21)$$

where $(\dot{\cdot})\equiv i(\partial/\partial t')$ and the coefficients a_n, b_n, etc., are given in Appendix C.

The quantity T_n^s is substituted from (6.20) in (6.21) and the result is used to eliminate X_{n-1}^s and X_{n+1}^s in (6.18) and (6.19) to yield

$$\mathbf{A}\dot{\mathbf{Y}}=\mathbf{B}\mathbf{Y}. \quad (6.22)$$

In Appendix C one finds a description of the matrices **A**, **B** and **Y** as well as the numerical method used to solve this matrix equation and the energetics of the model.

Multiplying (6.22) by the inverse of **A** we have

$$\dot{\mathbf{Y}}=\mathbf{A}^{-1}\mathbf{B}\mathbf{Y}.$$

Then by letting $\mathbf{C}=\mathbf{A}^{-1}\mathbf{B}$ and $\mathbf{Y}(t')=e^{-i\sigma t'}\mathbf{W}$ we obtain

$$(\mathbf{C}-\sigma\mathbf{I})\mathbf{W}=0, \tag{6.23}$$

which becomes an ordinary eigenvalue-eigenfunction problem for σ if ω, Λ, s and S have assigned values. The frequency σ is a complex quantity ($\sigma=\lambda+i\nu$). The quantity λ is the real part of the frequency and ν is the exponential growth rate. The cases $\nu>0$ are associated with unstable modes, $\nu=0$ with neutral modes, and $\nu<0$ with decaying modes. The e-folding time in days is equal to $(4\pi\nu)^{-1}$. Because the matrix $\mathbf{C}$ is real, for each complex eigenvalue σ, its complex conjugate σ^* is also a solution. Eq. (6.23) comprises two separate matrix systems with regard to the symmetry of the solutions, as even or odd functions of $\mu=\sin$ (latitude).

d. Discussion of the results

Figs. 22a and 22b (for streamfunctions symmetric and antisymmetric about the equator, respectively) present the growth rate of the unstable modes as a function of the discrete zonal wavenumber s and the mean meridional wavenumber m (defined as the number of zeros between the equator and pole of the real part of Φ_1' plus 1) for $S=0.005$ (corresponding to $\theta_{s_1}-\theta_{s_3}\approx 37$ K) and $\omega=\Lambda=0.01$ [corresponding to $\bar{U}$ (200 mb)$-\bar{U}$ (700 mb)≈ 13 m s^{-1} in mid-latitudes]. The lower layer basic wind is taken equal to zero. Both systems $\gamma=1$ and $\gamma=0$ are shown for comparison. The maximum growth rate for this case is seen to be for $s=4$ and $m=3$ with corresponding eigenfunctions having streamfunction (ψ) symmetric about the equator.

Fig. 23a displays the amplitudes and phases of the eigenfunctions Φ_1' and Φ_3' for the most unstable mode ($s=4$, $m=3$) shown in Fig. 22a for $\gamma=1$. Fig. 23b presents the corresponding momentum and heat transports by the baroclinic eddies. Figs. 24a and 24b are the counterpart of Figs. 23a and 23b for $\gamma=0$. The two solutions are remarkably alike, except that the amplitude of Φ_3' and $\overline{U_3'V_3'^*}\cos^2(\text{lat})$ in the lower layer (level 3) are relatively larger for $\gamma=0$.

The $\bar{U}\propto\cos(\text{lat})$ profile on a sphere is, in some ways, an analog of $\bar{U}=$constant on a β-plane. It is the simplest profile for a baroclinic instability study on a sphere, since it is always stable to barotropic disturbances.

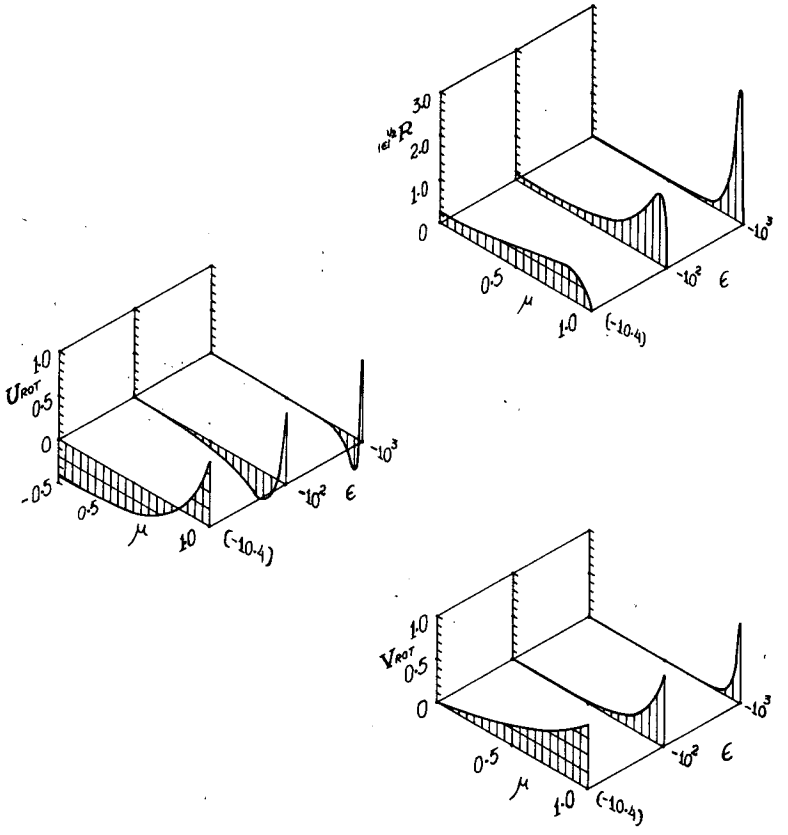

FIG. 17. As in Fig. 13 except for the balance equations for the "Burger 0" mode ($\epsilon<0$), with $s=1$. The cross-hatched eigenfunctions correspond to the limiting ($\lambda\to\infty$; $\epsilon<0$) solutions. At low frequencies, this mode agrees with the limiting type 6 solutions by Longuet-Higgins.

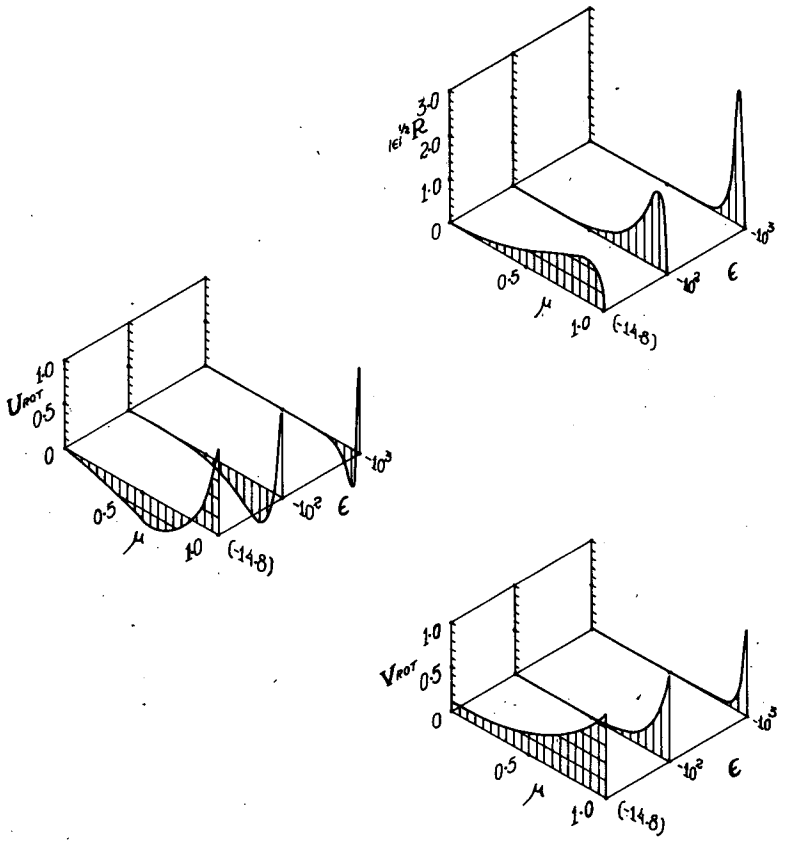

FIG. 18. As in Fig. 17 except for the "Burger 1" ($\epsilon<0$) mode.

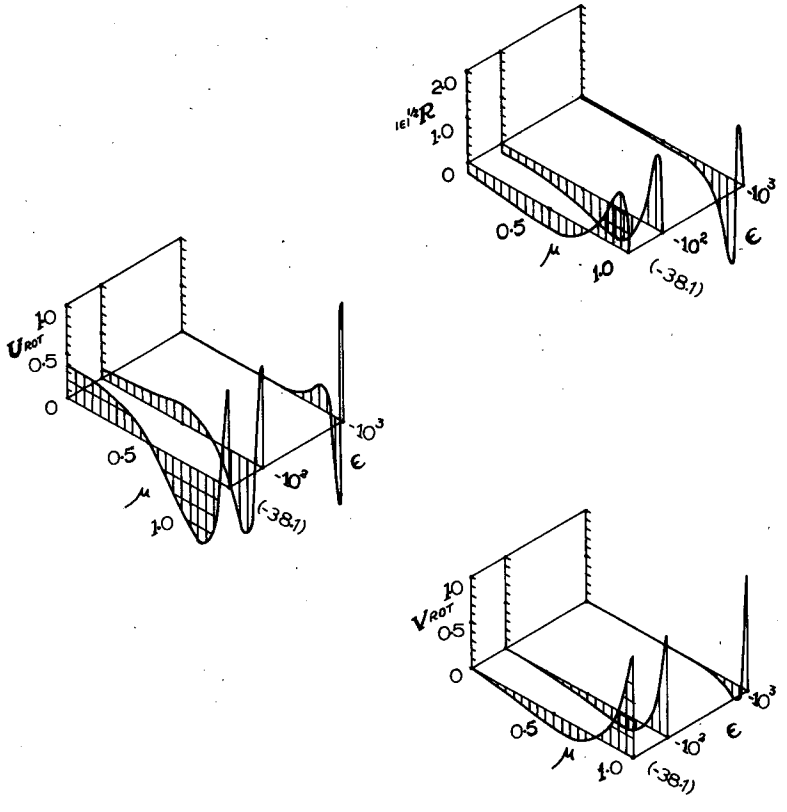

FIG. 19. As in Fig. 17 except for the "Burger 2" ($\epsilon<0$) mode.

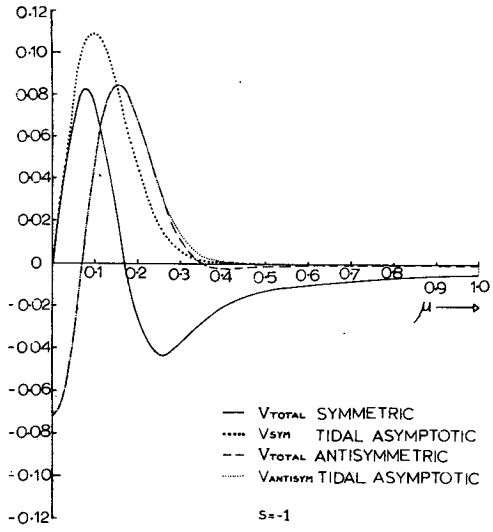

FIG. 20. Comparison of the total meridional velocity (V_{total}) of the balance equations with the asymptotic solutions of type 2 for $s=-1$ described by Longuet-Higgins. The discrepancy between the V_{total} Symmetric of the balance equations for $\epsilon=1.07\times10^{4}$, $\lambda=1.97\times10^{-3}$, and the asymptotic solution of type 2 for $\epsilon=1.07\times10^{4}$ and $\nu=1$ is shown. The good agreement between the V_{total} Antisymmetric of the balance equations for $\epsilon=1.02\times10^{4}$, $\lambda=1.95\times10^{-3}$ and the type 2 solution for $\epsilon=1.02\times10^{4}$ and $\nu=2$ is also shown.

The most unstable perturbations for $\bar{U}=$ constant on a β-plane analysis give no net transport of momentum across latitude circles, as shown by Phillips (1954). Our results, however, show a momentum transport $[\overline{u_1'v_1'^*}\cos^2(\text{lat})$ and $\overline{u_3'v_3'^*}\cos^2(\text{lat})]$ poleward for all latitudes (Fig. 24b), even when $\bar{U}$ is in solid rotation at each level. The effects of spherical geometry are evidently very important in this case. The ratio $\max \overline{u_1'v_1'^*}\cos^2(51°)/\max \overline{v_2T_2^*}\cos(60°)$ is approximately

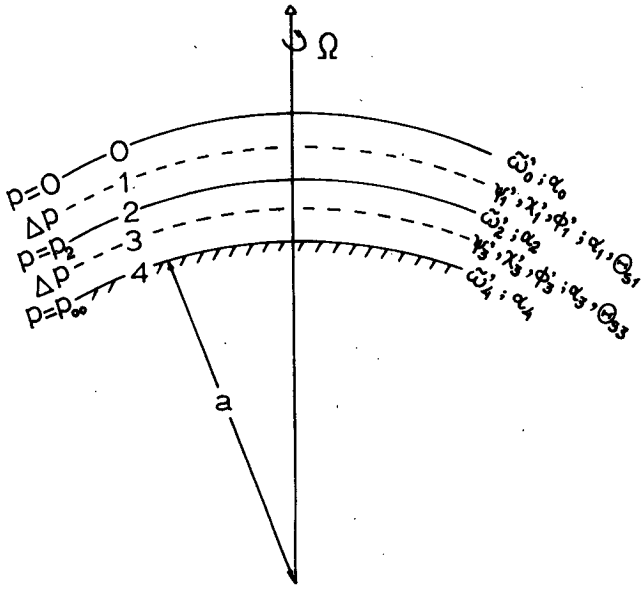

FIG. 21. Scheme of a two-layer model.

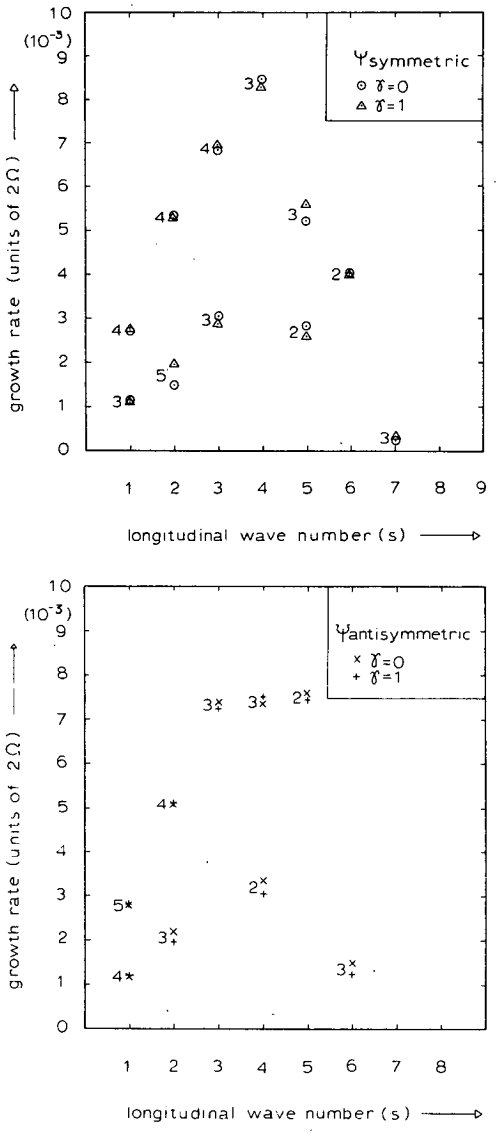

FIG. 22. Growth rates (units of 2Ω) for the unstable solutions with streamfunction symmetric (a) and antisymmetric (b) about the equator as a function of the longitudinal wavenumber (s) and the meridional modal number (m) [shown on the left of the circles and triangles] for the $\bar{U}\propto\cos$ (lat) profile. The values obtained using the two set of equations ($\gamma=0, \gamma=1$) are shown for comparison. Numerical values of the parameters are $S=0.005$, $\omega=\Lambda=0.01$.

1.6 m s^{-1} °C^{-1}, while the observed ratio (mean annual values) $\max \overline{u_1'v_1'^*}\cos^2(35°)/\max \overline{v'T'^*}\cos(50°)$ is approximately 1.56 m s^{-1} °C^{-1} (Oort and Rasmusson, 1971).

Further study using the model developed in this section to answer questions concerning the effects of spherical geometry on baroclinic instability will be presented in Moura and Stone (1975).

7. Modified balance equations

Our study of the linearized balance equations has shown a significant discrepancy between the symmetric equatorial Rossby modes as described by the balance

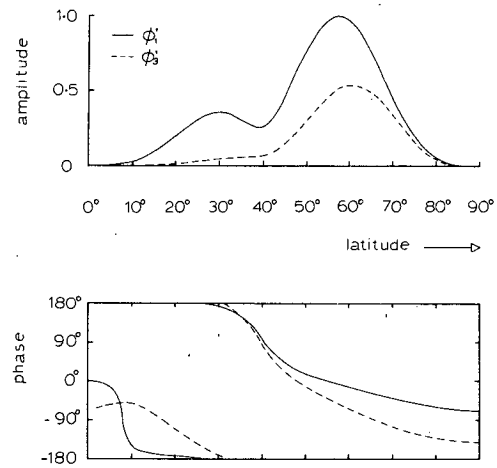

FIG. 23a. Eigenfunctions Φ_1 and Φ_3 for the most unstable mode for the profile $\bar{U} \propto \cos$ (lat), using the balance equations ($\gamma=1$). Numerical values of the parameters are: $S=0.005$; $\omega=\Lambda=0.01$. This mode has $\sigma=-0.03145+i\,0.008280$, $s=4$, $m=3$ and sym$=0$ (symmetric streamfunction).

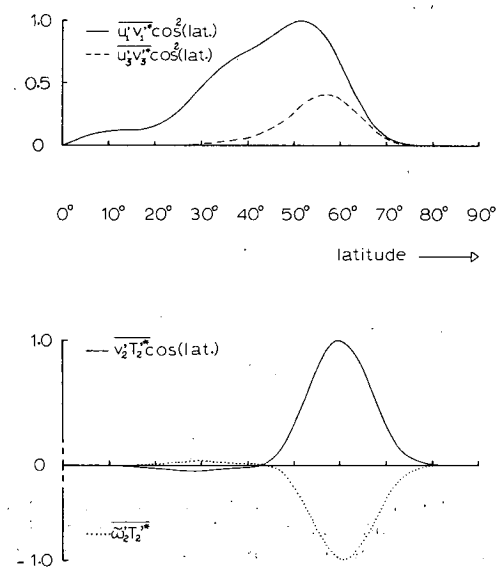

FIG. 23b. Angular momentum and heat transports corresponding to Fig. 23a.

equations and the same modes (type 2) as described by the LTE (Section 3). A closer examination of this problem reveals that a very good description of these modes can be obtained by keeping the α term ($\alpha=1$) in the original equation of balance [Eqs. (2.8) or (3.3)]. The system of equations (2.7)–(2.10) with $\alpha=1$ is also energetically consistent and will be denoted "modified balance equations." Charney's (1962) scale analysis has shown that the magnitude of this α term depends on the parameter $E=\mathrm{Ro}^{-2}\mathrm{Ri}^{-1}$, where Ro is the Rossby number and Ri a Richardson number. For $E=O(1)$ (typical of synoptic-scale atmospheric motions), the α term appears as a first-order term in an expansion in powers of Ro; it is therefore smaller than the other important terms if the horizontal scale is small compared to the earth's radius.

a. Discussion of the results

Fig. 25 shows the eigenvalues for $s=1$. The inclusion of the $\alpha=1$ term allows for eastward moving waves with $\epsilon>0$, which were not present in the balance equations. The integral expression (4.2) shows that this is true only for those modes with

$$\int_{-1}^{+1}|Q|^2d\mu > \int_{-1}^{+1}|P|^2d\mu,$$

i.e., modes with very significant divergence compared

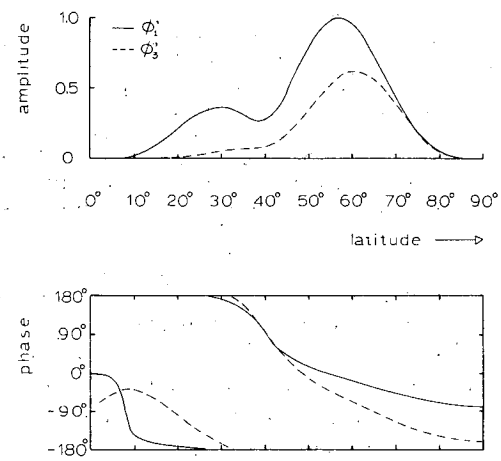

FIG. 24a. As in Fig. 23a except for $\gamma=0$. This mode has $\sigma=-0.03132+i\,0.008424$; $s=4$, $m=3$, sym$=0$.

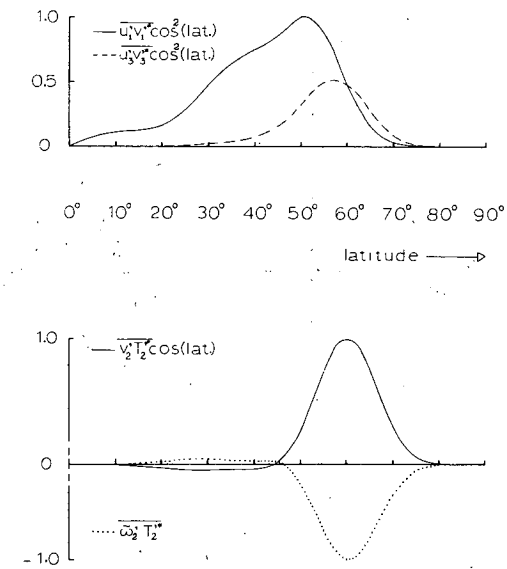

FIG. 24b. As in Fig. 23b.

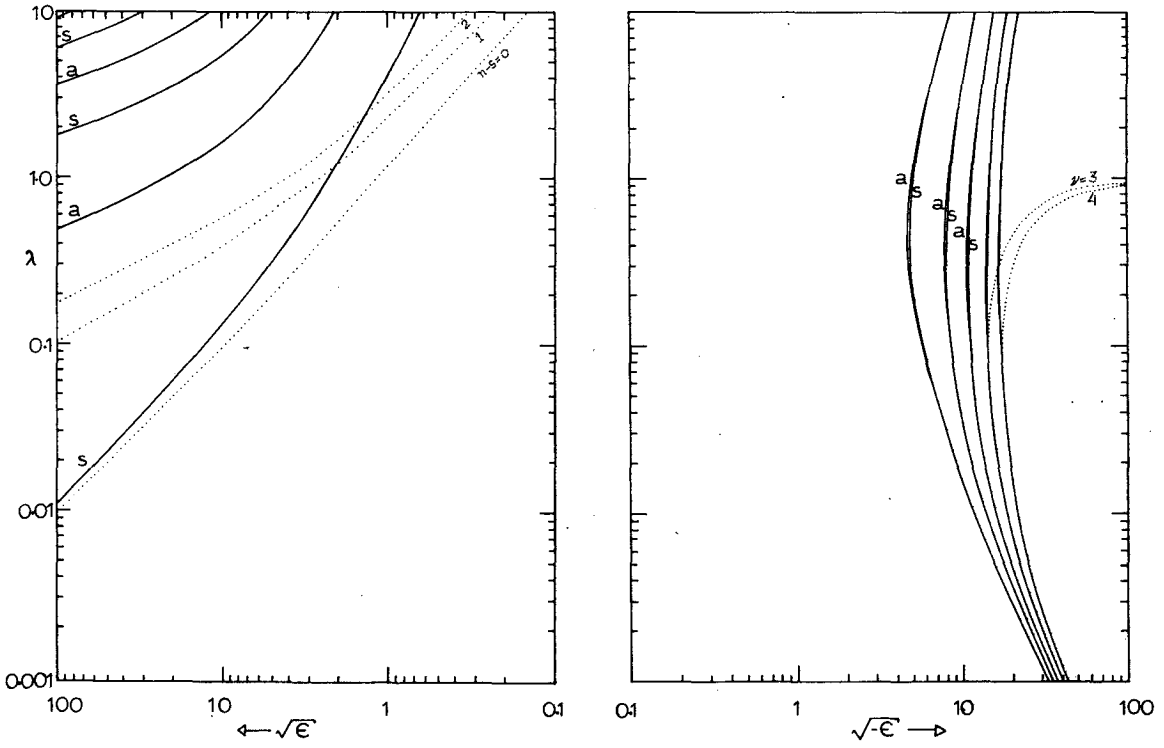

FIG. 25. Eigenvalues for the "modified balance equations" for the longitudinal wavenumber $s=1$. The figure shows high-frequency eastward propagating waves for ϵ positive. The equatorial Kelvin mode agrees well with Longuet-Higgins' results (dotted lines) at large ϵ. For negative values of ϵ and low frequencies, the "Burger" modes agree well with Longuet-Higgins' type 6. At large frequencies, however, they bend toward higher values of $-\epsilon$, but still do not accumulate at $\lambda=1$. (Compare with Figs. 4 and 8.)

to their vorticity, over the whole globe. The modes for $\epsilon>0$ have frequencies much higher than the corresponding ones for the LTE, with exception of the "Kelvin mode," where the agreement is better at large ϵ. As $\epsilon\to+0$ the modes numerically approach the asymptote $\lambda\epsilon=n^2(n+1)^2/s$.

For $\epsilon<0$, the limiting solutions $\lambda\approx s/(-\epsilon)$ [Eq. (4.11)] as $\epsilon\to-\infty$ are also solutions to the modified balance equations, with a better pairing [described by (4.11)] between symmetric and antisymmetric modes as compared to Fig. 8. As λ is increased, the modes bend toward higher values of $(-\epsilon)$, instead of continuing straight upward as they do for the balance equations (see Fig. 8). However they still do not accumulate at $\lambda=1$.

Fig. 26 is the counterpart of Fig. 9 for the modified balance equations for $s=-1$. The symmetric Rossby modes now also agree very well with Longuet-Higgins' results (compare also with Fig. 5), but the "mixed Rossby-gravity" mode still has too large a frequency as ϵ is increased. The solutions $\lambda\to\infty$ for finite $\epsilon<0$ of the balance equations (Section 4), corresponding to the modes continuing straight upward in Figs. 6 and 9, are changed so as to bend back toward small values of $-\epsilon$, as λ increases. They are numerically asymptotic to $\lambda\epsilon=n^2(n+1)^2/s$, which is the value of $\lambda\epsilon$ that makes the coefficient of A_n^s vanish in expression (B10). [This occurs for $s<0$ and $\epsilon<0$ and also for $s>0$ and $\epsilon>0$.]

For $s=0$, the eigenvalues of the modified balance equations are the same as those of the balance equations (Fig. 7). This is explained by (4.2).

Fig. 27 shows the excellent agreement between the total meridional velocities $[(1-\mu^2)^{\frac{1}{2}}(dQ/d\mu)+s/(1-\mu^2)^{\frac{1}{2}}P]$ in the first two "Rossby equatorial modes" as described by the modified balance equations and the corresponding asymptotic expression (3.7) from Longuet-Higgins' study. (Compare with Fig. 20.)

b. Kelvin wave solution

The equatorial Kelvin wave solution of the LTE for large ϵ can be approximately described by the modified balance equations, as shown by our computations (see Fig. 25). Fig. 28 shows U_T, $\epsilon^{\frac{1}{2}}R$ and V_T at a large value of ϵ from our calculations for this mode. The balance between U_T and $\epsilon^{\frac{1}{2}}R$ is approximate with error typical of $O(\epsilon^{-\frac{1}{2}})$. An expansion in powers of $\epsilon^{-\frac{1}{2}}$ for large ϵ elucidates the approximation.

Let us return to Eqs. (3.2)–(3.4) with $\alpha'=0$ and $\alpha=1$ and define

$$V=(1-\mu^2)(dQ/d\mu)+sP$$

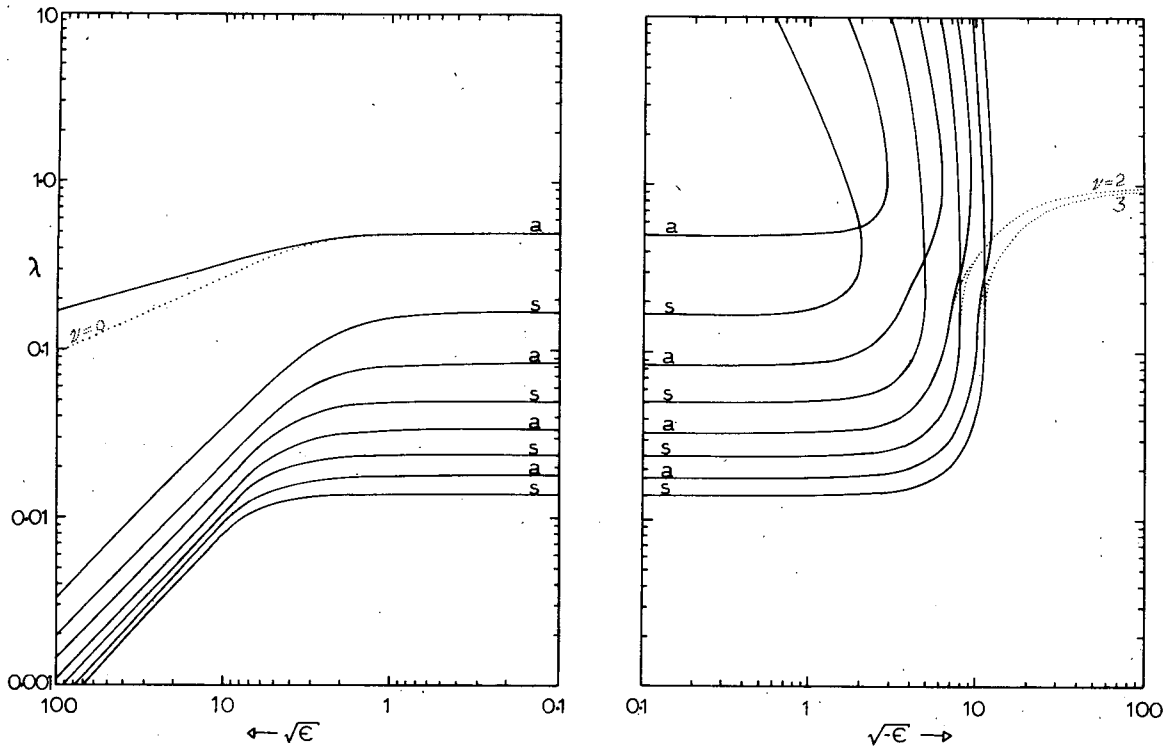

FIG. 26. As in Fig. 25 except for $s=-1$. All the equatorial Rossby modes agree well with Longuet-Higgins' type 2. The westward moving part of the mixed Rossby-gravity mode has too high a frequency when compared with Longuet-Higgins' results (dotted lines). For negative values of ϵ, the modes bend back toward small values of $-\epsilon$, asymptotically to $\lambda\sim n^2(n+1)^2/(s\epsilon)$.

and

$$U=-[(1-\mu^2)(dP/d\mu)+sQ].$$

Since the numerical solution appears equatorially trapped, we change the coordinate to $\mu=\epsilon^{-\frac{1}{4}}\eta$ [$\eta=O(1)$] and expand the variables as follows:

$$\left.\begin{aligned}\lambda&=\epsilon^{-\frac{1}{2}}s(\lambda_0+\epsilon^{-\frac{1}{2}}\lambda_1+\cdots)\\ U&=(U_0+\epsilon^{-\frac{1}{2}}U_1+\cdots)\\ R&=\epsilon^{-\frac{1}{2}}(R_0+\epsilon^{-\frac{1}{2}}R_1+\cdots)\\ V&=\epsilon^{-\frac{1}{4}}s(0+\epsilon^{-\frac{1}{2}}V_1+\cdots)\end{aligned}\right\}. \tag{7.1}$$

The zeroth order solution is

$$\left.\begin{aligned}\lambda_0&=1\\ U_0&=R_0\propto\exp(-\eta^2/2)\end{aligned}\right\}. \tag{7.2}$$

This zeroth order result is the same for the LTE [see (3.8)]. The first order equations can be combined to give the following equation for V_1:

$$(d^2/d\eta^2)[(d/d\eta)-\eta]V_1=(d^2/d\eta^2)(2\lambda_1-\eta^2)\times\exp(-\eta^2/2)+s^2\exp(-\eta^2/2). \tag{7.3}$$

If a similar expansion is made using the LTE instead, one also obtains (7.3) but without the last term in the right-hand side. This term forces V_1 to have significant amplitude away from equatorial regions, which cannot be described by the asymptotic relation (3.8) for v.

c. Asymptotic solutions as $\epsilon\rightarrow\pm 0$

In addition to Hough's waves of the second class, there are other solutions to the modified balance equations as $\epsilon\rightarrow+0$ (eastward-moving waves) and as $\epsilon\rightarrow-0$ (westward-moving waves). Our computations of the eigenvalues (Figs. 26 and 25) have revealed the existence of asymptotic solutions $\lambda\epsilon\approx n^2(n+1)^2/s$, which makes the coefficient of A_n^s in (B6) vanish. To study this possibility we take (3.2)–(3.4) with $\alpha=1$ and $\alpha'=0$ and make the following expansion:

$$\left.\begin{aligned}\lambda&=\epsilon^{-1}(\lambda_0+\epsilon\lambda_1+\cdots)\\ P&=(P_0+\epsilon P_1+\cdots)\\ Q&=(Q_0+\epsilon Q_1+\cdots)\\ R&=(R_0+\epsilon R_1+\cdots)\end{aligned}\right\}. \tag{7.4}$$

Collecting the zeroth order terms ($\epsilon\rightarrow+0$), we obtain

$$\left.\begin{aligned}P_0&\equiv 0\\ R_0&=P_n^{|s|}(\mu)\\ Q_0&=-[n(n+1)/s]P_n^{|s|}(\mu)\\ \lambda_0&=n^2(n+1)^2/s,\quad s>0\end{aligned}\right\}. \tag{7.5}$$

These physically unrealistic solutions have very high frequency ($\lambda\approx\epsilon^{-1}$), even when compared to the frequency of the first class waves (Section 3). [Note that the solutions (7.5) also apply to $\epsilon\rightarrow-0$, but for

negative values of s.] Large λ of course makes it unrealistic to neglect the α' term in (3.3).

In closing this section we shall compare the balance equations with the modified balance equation with respect to their numerical practicability using a numerical model.

Suppose we want to integrate (2.7)–(2.10) numerically with the forcing (**F**) and heating (q) given and with the proper boundary conditions. Given ψ_0 (or Φ_0) at $t=0$ we then calculate Φ_0 (or ψ_0) from (2.8) if $\alpha=0$ [the ellipticity condition must be satisfied; see Houghton (1968)]. With ψ_0 and Φ_0 known, Eqs. (2.7), (2.9) and (2.10) contain the four unknowns $\partial\psi/\partial t$, χ, $\dot{Z}$, $\partial\Phi/\partial t$, at $t=0$. The fourth equation relating $\partial\psi/\partial t$ and $\partial\Phi/\partial t$ is obtained by taking the time derivative of (2.8). Once $\partial\psi/\partial t$ and $\partial\Phi/\partial t$ are calculated, $\psi_{\Delta t}$ and $\Phi_{\Delta t}$ are obtained at $t=\Delta t$ (say by a forward time extrapolation). [Charney (1962) has integrated these equations through an iterative scheme for a homogeneous incompressible ocean.]

This procedure is of no use in the case $\alpha=1$. Now Φ_0 (or ψ_0) cannot be calculated from ψ_0 (or Φ_0) by means of (2.8) and the initial condition is incomplete. One could try to get around this difficulty in an iterative manner. Suppose ψ_0 is given at $t=0$; one can solve the equations with $\alpha=0$ as explained above, to get $\partial\psi/\partial t$, $\partial\Phi/\partial t$, χ and $\dot{Z}$ at $t=0$. Now that χ is known, we can go back to (2.8) with $\alpha=1$ and evaluate a new value for Φ_0 from ψ_0 and χ. Eq. (2.9) is then used to get a new estimate of $\partial\Phi/\partial t$ at $t=0$. An iteration could then be performed. Once $\Phi_{\Delta t}$ and $\psi_{\Delta t}$ are known at $t=\Delta t$, from this time on, one could solve (2.8) for χ and march in time. It is possible that one runs into a problem of truncation error. If Φ and ψ are a well-balanced field, χ is a small quantity and may be "contaminated" by truncation errors. This scheme might allow for motions with more divergence without describing the spurious high-frequency free solutions. [If Φ_0 is given instead of ψ_0 at $t=0$, one goes into the same procedure as outlined above, but in addition, a new estimate of $\partial\Phi/\partial t$ at $t=0$ has to be calculated using (2.7)].

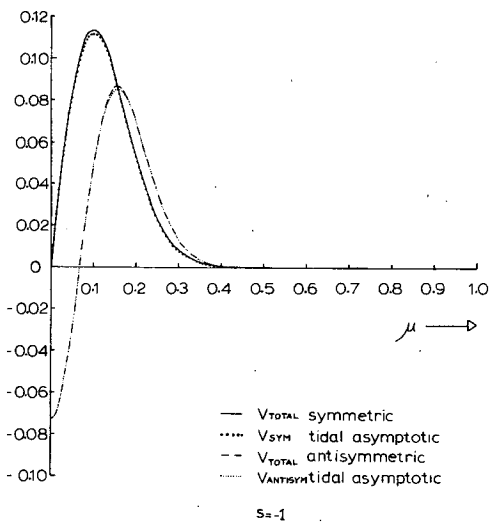

FIG. 27. Comparison of the total meridional (V_{total}) velocity of the "modified balance equations" with the asymptotic solutions of type 2 for $s=-1$ described by Longuet-Higgins. The agreement between the V_{total} Symmetric for $\epsilon=0.956\times10^4$ and the V_{total} Antisymmetric for $\epsilon=1.03\times10^4$ with their respective asymptotic solutions of type 2 ($\nu=1$, and $\nu=2$) is very good. (Compare with Fig. 20.)

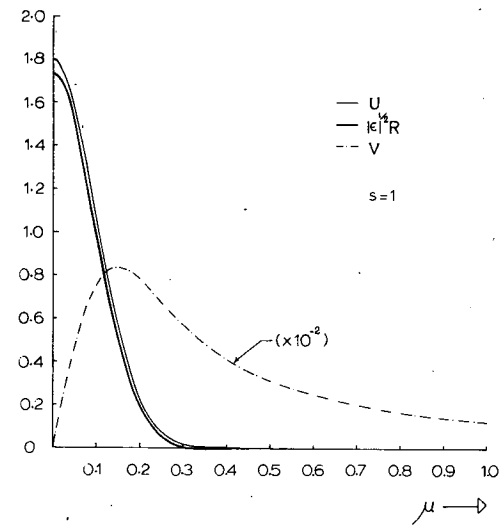

FIG. 28. Eigenfunctions $|\epsilon|^{\frac{1}{4}}R$ and total zonal and meridional velocities for the equatorial Kelvin mode as described by the "modified balance equations" for $\epsilon=1.01\times10^4$, $\lambda=1.09\times10^{-2}$, and $s=1$.

The main virtue of the balance equations (i.e., that they are able to describe motions without gravity waves) is no longer true for the modified balance equations. Since the latter ones admit high-frequency, free mode solutions, these modes might require the use of shorter time steps. Therefore, if one does not devise an efficient method to get rid of these high-frequency modes, it will seem hardly acceptable to use these equations in numerical models for practical purposes.

8. Concluding remarks

Our study of the linearized balance equations has shown that they describe well the slow, large-scale motions in the atmosphere. Their major drawback is in not describing the equatorial Kelvin wave observed by Wallace and Kousky (1968). Topographic forcing in an easterly flow at equatorial latitude excites the vertically propagating Kelvin wave as the main response (Webster, 1972). In this case, the balance equations will have a wrong response: the polarly trapped modes, which are also vertically trapped, are the most excited.

The "modified balance equations," on the other hand, have been shown to be able to describe this Kelvin wave solution. But, unfortunately, they also describe spurious high-frequency free solutions. To

avoid these solutions, we have proposed a tentative iterative scheme to integrate these equations. Professor Jule Charney (private communication) has shown that this scheme works well for a simple mid-latitude β-plane analysis. But, to show that one can get the Kelvin wave in an equatorial analysis, more work needs to be done.

The results of a numerical two-layer model used in a a baroclinic instability study have indicated a remarkable similarity of the solutions obtained by using either the balance equations or the quasi-geostrophic equations over a sphere, for realistic values of the parameters involved.

Acknowledgments. The author expresses his gratitude to Professor Norman Phillips for serving as thesis advisor throughout this investigation. Thanks are also due to Professors Jule Charney, Richard Lindzen, John Young and Peter Stone for many stimulating discussions. Funding was provided by the Instituto de Pesquisas Espaciais (INPE), Brazil. Additional financial support was provided by a NASA International Fellowship and by the National Science Foundation under Grant GA 28724.

APPENDIX A

List of Symbols

a	earth's mean radius
Ω	earth's rate of rotation
g	acceleration due to gravity
$\mathcal{R}$	gas constant for dry air
z	height
p	pressure (p_0, reference pressure)
T	temperature
ρ	density
Θ	potential temperature
Θ_s	potential temperature for a standard atmosphere
Z	vertical coordinate $[=-\ln(p/p_0)]$
t	time
θ	colatitude
μ	$\cos\theta$
f	Coriolis parameter $[=2\Omega\mu]$
β	derivative of the Coriolis parameter evaluated at a fixed latitude
ϕ	longitude
Φ	geopotential $[=gz]$
$\tilde{S}$	static stability
N^2	(Brunt-Väisälä frequency)^2
s	longitudinal wavenumber
n	modal number
σ	frequency
λ	nondimensional frequency $[=\sigma/2\Omega]$
ν	growth rate (also a modal index)
ψ	streamfunction
χ	velocity potential
ζ	vertical component of the relative vorticity
$\nabla^2\chi$	divergence of the horizontal motion
$\tilde{\omega}$	vertical p-velocity $[=Dp/Dt]$
$\dot{Z}$	vertical Z-velocity $[=DZ/Dt=-\tilde{\omega}/p]$
q	rate of heating
$\mathbf{F}$	horizontal component of frictional force
$\hat{\mathbf{i}}, \hat{\mathbf{j}}, \hat{\mathbf{k}}$	unit vectors toward the east, north, vertical
c^2	separation constant
ϵ	Lamb's parameter $[=4\Omega^2a^2/c^2]$
P, Q, R	latitudinal dependence of ψ, χ, Φ
$P_n^s(\mu)$	associated Legendre function of degree n and order s
$H_\nu(\eta)$	Hermite polynomial of degree ν
$L_\nu^{(k)}(\omega)$	generalized Laguerre polynomial of degree ν and order k
u	zonal velocity $\{=(1/a)[-(1-\mu^2)^{\frac{1}{2}}\partial\psi/\partial\mu+(1-\mu^2)^{-\frac{1}{2}}\partial\chi/\partial\phi]\}$
v	meridional velocity $\{=(1/a)[-(1-\mu^2)^{\frac{1}{2}}\partial\chi/\partial\mu+(1-\mu^2)^{-\frac{1}{2}}\partial\psi/\partial\phi\}$
U	"zonal velocity" $\{=-[(1-\mu^2)^{\frac{1}{2}}dP/d\mu+(1-\mu^2)^{-\frac{1}{2}}sQ]\}$
V	"meridional velocity" $\{=[(1-\mu^2)^{\frac{1}{2}}dQ/d\mu+(1-\mu^2)^{-\frac{1}{2}}sP]\}$
U_T	total zonal velocity
V_T	total meridional velocity
U_{rot}	rotational part of the zonal velocity $[=-(1-\mu^2)^{\frac{1}{2}}dP/d\mu]$
V_{rot}	rotational part of the meridional velocity $[=sP]$
η	stretched coordinates $=\epsilon^{\frac{1}{4}}\mu$
ω	stretched coordinates $=(-\epsilon)^{\frac{1}{4}}\theta$
α, α'	indices (0 or 1) used to indicate the balance approximation
δ, Λ, ω	parameters used in a two-layer model
γ	parameter (0 or 1)

APPENDIX B

Expansion in Surface Spherical Harmonics

The method used to solve the set of equations (3.2)–(3.4) is to expand $P(\mu)$ and $Q(\mu)$ in series of surface spherical harmonics. In doing so we use the convention $s\geqslant 0$, with λ possibly being negative, for computational convenience. The results are readily converted to the other convention of non-negative λ, with both positive and negative s (as shown in the figures). Then,

$$\left.\begin{aligned} P(\mu)&=\sum_{n=s}^{\infty} B_n^s P_n^s(\mu)\\ Q(\mu)&=\sum_{n=s}^{\infty} A_n^s P_n^s(\mu)\end{aligned}\right\}, \tag{B1}$$

where $P_n^s(\mu)$ is the associated Legendre function of degree n and order s [Korn and Korn, (1968), p. 870].

Eq. (3.4) becomes

$$R(\mu)=-(\lambda\epsilon)^{-1}\sum_{n=s}^{\infty} n(n+1)A_n^s P_n^s(\mu). \tag{B2}$$

The series (B1) and (B2) when put into (3.2) and (3.3) gives:

$$\sum_{n=s}^{\infty}\{\lambda n(n+1)B_n^sP_n^s-n(n+1)A_n^s\mu P_n^s+A_n^s(1-\mu^2)\times dP_n^s d\mu+sB_n^sP_n^s\}=0, \quad \text{(B3)}$$

$$\sum_{n=s}^{\infty}\{n(n+1)B_n^sP_n^s-B_n^s(1-\mu^2)dP_n^s/d\mu+n^2(n+1)^2/(\lambda\epsilon)A_n^sP_n^s-\alpha sA_n^sP_n^s\}=\alpha'\sum_{n=s}^{\infty}\{\lambda n(n+1)A_n^sP_n^s\}. \quad \text{(B4)}$$

The properties of P_n^s are used in (B3) and (B4), which then become (only the $\alpha'=0$ case is considered):

$$\{\lambda n(n+1)+s\}B_n^s-\{n(n+2)(n+s+1)/(2n+3)\}A_{n+1}^s-\{(n-1)(n+1)(n-s)/(2n-1)\}A_{n-1}^s=0, \quad \text{(B5)}$$

$$\{n^2(n+1)^2/(\lambda\epsilon)-\alpha s\}A_n^s=-\{n(n+2)(n+s+1)/(2n+3)\}B_{n+1}^s-\{(n-1)(n+1)(n-s)/(2n-1)\}B_{n-1}^s. \quad \text{(B6)}$$

We now substitute A_n^s from (B6) $[n^2(n+1)^2\neq\lambda\epsilon\alpha s]$ into (B5) to get

$$d_{n-2}B_{n-2}^s+(a_n+g_n+b_n-\lambda)B_n^s+c_{n+2}B_{n+2}^s=0, \quad \text{(B7)}$$

where:

$$d_n=e_{n+1}[n(n-s+1)(n-s+2)]/[(2n+1)(2n+3)(n+1)(n+2)^2]$$

$$a_n=e_{n+1}[n(n-s+1)(n+s+1)]/[(2n+1)(2n+3)(n+1)^3]$$

$$g_n=e_{n-1}[(n+1)(n-s)(n+s)]/[(2n-1)(2n+1)n^3]$$

$$b_n=-s/[n(n+1)]$$

$$c_n=e_{n-1}[(n+1)(n+s-1)(n+s)]/[(n-1)^2n(2n-1)(2n+1)]$$

$$e_n=\lambda\epsilon/[\alpha s\lambda\epsilon/(n^2(n+1)^2)-1]; \quad (\alpha=0 \text{ or } 1)$$

$(g_1=b_n=0$ for $s=0$, $g_n=0$ when $n=s$, $s=1, 2, \ldots)$.

There are two separate systems of equations described by (B7), which can be put in matrix form as follows:

$$\begin{bmatrix}(a_s+g_s+b_s-\lambda) & (c_{s+2}) & 0 & \cdots\\ (d_s) & (a_{s+2}+g_{s+2}+b_{s+2}-\lambda) & (c_{s+4}) & 0\cdots\\ 0 & (d_{s+2}) & (a_{s+4}+g_{s+4}+b_{s+4}-\lambda) & \cdots\\ \cdot & 0 & (d_{s+4}) & \\ \cdot & \cdot & \cdot & \text{etc.}\end{bmatrix}\begin{bmatrix}B_s^s\\ B_{s+2}^s\\ B_{s+4}^s\\ \cdot\\ \cdot\end{bmatrix}=\begin{bmatrix}0\\0\\0\\ \cdot\\ \cdot\end{bmatrix} \quad \text{(B9)}$$

$$\begin{bmatrix}(a_{s+1}+g_{s+1}+b_{s+1}-\lambda) & (c_{s+3}) & 0\cdots\\ (d_{s+1}) & (a_{s+3}+g_{s+3}+b_{s+3}-\lambda) & \cdots\\ 0 & (d_{s+3}) & \cdots\\ \cdot & 0 & \cdots\\ \cdot & \cdot & \text{etc.}\end{bmatrix}\begin{bmatrix}B_{s+1}^s\\ B_{s+3}^s\\ B_{s+5}^s\\ \cdot\\ \cdot\end{bmatrix}=\begin{bmatrix}0\\0\\0\\ \cdot\\ \cdot\end{bmatrix} \quad \text{(B10)}$$

For computations one has to truncate (B9) and (B10). An energetically consistent way to do this is to set either g or a equal to zero in the last diagonal element of (B9) or (B10), respectively (Moura, 1974). System (B9) [(B10)] with $n-s$ an even [odd] number correspond to motions for which P is an even [odd] function of μ, whereas Q and R are odd [even] functions of μ. These two tridiagonal systems may be solved by fixing values of s and of the product $\lambda\epsilon[n^2(n+1)^2\neq\lambda\epsilon\alpha s$ if $\alpha=1]$ and treating a simple eigenvalue problem for λ. In practice we have to truncate the infinite tridiagonal matrices and take the first $N\times N$ elements. Our computations (with double precision arithmetic) for $N=40$, when verified against those with $N=50$ have shown excellent agreement: the values of λ for $N=40$ and $N=50$ agree to 10 places for $|\lambda|\geq 10^{-3}$ and $|\epsilon|\leq 10^4$. Slower convergence occurs when the frequency is smaller than 0.001 for large positive ϵ (equatorial Rossby waves, Section 4b) and for large negative ϵ (Section 4b).

Once we obtain the eigenvectors B_n^s from (B9) and (B10) we calculate the corresponding A_n^s from (B6). The values of A_n^s and B_n^s are normalized in the following way, consistent with the normalization used by Longuet-Higgins (1968). Let E be the total energy (solenoidal kinetic+potential), i.e.,

$$E=\int_{-1}^{+1}\int_0^{2\pi}\tfrac{1}{2}[\nabla\Psi\cdot\nabla\Psi+(1/c^2)\Phi^2]a^2d\mu d\phi. \quad \text{(B11)}$$

Since $\{\Psi,\Phi\}=\mathrm{Re}\{[P(\mu),2\Omega R(\mu)]\exp(is\phi-i\sigma t)\}$, we have

$$E=\pi/2\left\{\int_{-1}^{+1}(1-\mu^2)|dP/d\mu|^2d\mu+s^2\int_{-1}^{+1}|R|^2/(1-\mu^2)d\mu+\epsilon\int_{-1}^{+1}|P|^2d\mu\right\}.$$

The choice $E=\pi/2$ implies that

$$s^2I_2+I_3+|\epsilon|I_4=1, \tag{B12}$$

where I_2, I_3, I_4 are the integrals defined in (4.3), and the absolute value of ϵ is taken for the $\epsilon<0$ modes (Longuet-Higgins). When (B1) and (B2) are used in (B12) the normalized A_n^s and B_n^s ensure that

$$\sum_{n=s}^{\infty}\{(n+s)!n(n+1)/[(n+\tfrac{1}{2})(n-s)!]\}\times\{(\lambda\epsilon)^{-2}|\epsilon|n(n+1)(A_n^s)^2+(B_n^s)^2\}=1. \tag{B13}$$

A similar relation is imposed for the truncated matrices used in computation (Moura, 1974).

The eigenfunctions are all defined in terms of the normalized A_n^s and B_n^s. Truncated series of spherical harmonics are used to compute $P(\mu)$, $Q(\mu)$ and $R(\mu)$ using (B1) and (B2). Other variables are then derived from $P(\mu)$, $Q(\mu)$ and $R(\mu)$:

Meridional velocity V

$$V=(1-\mu^2)^{\frac{1}{2}}dQ/d\mu+s(1-\mu^2)^{-\frac{1}{2}}P$$
$$=\sum_{n=s}^{N}[sB_n^s+(n+2)(n+s+1)/(2n+3)A_{n+1}^s$$
$$-(n-1)(n-s)/(2n-1)A_{n-1}^s](1-\mu^2)^{-\frac{1}{2}}P_n^s \tag{B14}$$

Zonal velocity U

$$U=-(1-\mu^2)^{\frac{1}{2}}dP/d\mu-s(1-\mu^2)^{-\frac{1}{2}}Q$$
$$=-\sum_{n=s}^{N}[sA_n^s+(n+2)(n+s+1)/(2n+3)B_{n+1}^s$$
$$-(n-1)(n-s)/(2n-1)B_{n-1}^s](1-\mu^2)^{-\frac{1}{2}}P_n^s \tag{B15}$$

Geopotential

$$R=-(\lambda\epsilon)^{-1}\sum_{n=s}^{N}n(n+1)A_n^sP_n^s(\mu). \tag{B16}$$

The rotational part of V and U in (B14) and (B15) are obtained by omitting the A terms in the respective series. It is these which form the major displays in Figs. 11–19.

APPENDIX C

Numerical Solution of the Matrix Equation $\mathbf{A\dot{Y}=BY}$ for $\delta=0$

The solution of the system of equations (6.11)–(6.14) is obtained through the truncated expansion (6.17), resulting in the set of algebraic equations (6.18)–(6.21), where

$$\left.\begin{array}{ll} a_n=(n-1)(n-s)/\{n(2n-1)\}, & b_n=(n+2)(n+s+1)/[(n+1)(2n+3)] \\ c_n=s\Lambda(n-s)/(2n-1), & d_n=s\Lambda(n+s+1)/(2n+3) \\ e_n=-s(1+2\omega)/[n(n+1)], & f_n=s\Lambda\{1-2/[n(n+1)]\} \\ w_n=(1+2\gamma\Lambda)/[n(n+1)S], & \Gamma_n=2\gamma\Lambda/[n(n+1)S] \\ A_n=\gamma\Lambda(n+2)a_n, & B_n=\gamma\Lambda(n-1)b_n \\ C_n=(1+2\gamma\omega)a_n, & D_n=(1+2\gamma\omega)b_n \end{array}\right\}. \tag{C1}$$

We eliminate T_n^s between (6.20) and (6.21) to get

$$w_n(a_n\dot{\Theta}_{n-1}^s+b_n\dot{\Theta}_{n+1}^s)+\Gamma_n(a_n\dot{\Psi}_{n-1}^s+b_n\dot{\Psi}_{n+1}^s)=-w_n(c_n\Psi_{n-1}^s+d_n\Psi_{n+1}^s)-X_n^s. \tag{C2}$$

We now use (C.2) to eliminate X_{n-1}^s and X_{n+1}^s from (6.19) and (6.18) which result in the following two equations:

$$C_nw_{n-1}a_{n-1}\dot{\Theta}_{n-2}^s+C_n\Gamma_{n-1}a_{n-1}\dot{\Psi}_{n-2}^s+(1+C_nw_{n-1}b_{n-1}+D_nw_{n+1}a_{n+1})\dot{\Theta}_n^s+(C_n\Gamma_{n-1}b_{n-1}+D_n\Gamma_{n+1}a_{n+1})\dot{\Psi}_n^s+$$
$$+D_nw_{n+1}b_{n+1}\dot{\Theta}_{n+2}^s+D_n\Gamma_{n+1}b_{n+1}\dot{\Psi}_{n+2}^s=-w_{n-1}c_{n-1}\Psi_{n-2}^s+e_n\Theta_n^s+(f_n-C_nw_{n-1}d_{n-1}-D_nw_{n+1}c_{n+1})\Psi_n^s$$
$$-D_nw_{n+1}d_{n+1}\Psi_{n+2}^s \tag{C3}$$

$$A_nw_{n-1}a_{n-1}\dot{\Theta}_{n-2}^s+A_n\Gamma_{n-1}a_{n-1}\dot{\Psi}_{n-2}^s+(A_nw_{n-1}b_{n-1}-B_nw_{n+1}a_{n+1})\dot{\Theta}_n^s+(1+A_n\Gamma_{n-1}b_{n-1}-B_n\Gamma_{n+1}a_{n+1})\dot{\Psi}_n^s$$
$$-B_nw_{n+1}b_{n+1}\dot{\Theta}_{n+2}^s-B_n\Gamma_{n+1}b_{n+1}\dot{\Psi}_{n+2}^s=-w_{n-1}c_{n-1}\Psi_{n-2}^s+f_n\Theta_n^s$$
$$+(e_n-A_nw_{n-1}d_{n-1}+B_nw_{n+1}c_{n+1})\Psi_n^s+B_nw_{n+1}d_{n+1}\Psi_{n+2}^s. \tag{C4}$$

The system of equations (C3)–(C4) separates into two symmetries. One for $n=s,\ s+2,\ s+4,\ \ldots,(N-1)$ and the other for $n=s+1,\ s+3,\ \ldots,\ N$.

Let us write (C3)–(C4) in matrix form

$$\mathbf{A\dot{Y}=BY}, \tag{C5}$$

where the matrices $\mathbf{Y}$, $\mathbf{A}$, and $\mathbf{B}$ are as follows:

$$\mathbf{Y}=\begin{bmatrix}\Theta_j^s\\ \Psi_j^s\\ \Theta_{j+2}^s\\ \Psi_{j+2}^s\\ \cdot\end{bmatrix};\quad j=s \text{ or } j=s+1.$$

Matrix **A** ($j=s$ or $j=s+1$).

Banded matrix with bandwidth 7. The underlined terms are equal to zero when $j=s$.

$$\begin{bmatrix}
(1+D_jw_{j+1}a_{j+1}+\underline{C_jw_{j-1}b_{j-1}}) & (C_j\Gamma_{j-1}b_{j-1}+D_j\Gamma_{j+1}a_{j+1}) & (D_jw_{j+1}b_{j+1}) & (D_j\Gamma_{j+1}b_{j+1} & 0 & \cdots & \\
(-B_jw_{j+1}a_{j+1}+\underline{A_jw_{j-1}b_{j-1}}) & (1+\underline{A_j\Gamma_{j-1}b_{j-1}}-B_j\Gamma_{j+1}a_{j+1}) & (-B_jw_{j+1}b_{j+1}) & (-B_j\Gamma_{j+1}b_{j+1}) & 0 & \cdots & \\
(C_{j+2}w_{j+1}a_{j+1}) & (C_{j+2}\Gamma_{j+1}a_{j+1}) & (1+D_{j+2}w_{j+3}a_{j+3}+C_{j+2}w_{j+1}b_{j+1}) & (C_{j+2}\Gamma_{j+1}b_{j+1}+D_{j+2}\Gamma_{j+3}a_{j+3}) & (D_{j+2}w_{j+3}b_{j+3}) & (D_{j+2}\Gamma_{j+3}b_{j+3}) & 0\cdots \\
(A_{j+2}w_{j+1}a_{j+1}) & (A_{j+2}\Gamma_{j+1}a_{j+1}) & (-B_{j+2}w_{j+1}a_{j+3}+A_{j+2}w_{j+1}b_{j+1}) & (1+A_{j+2}\Gamma_{j+1}b_{j+1}-B_{j+2}\Gamma_{j+3}a_{j+3}) & (-B_{j+2}w_{j+3}b_{j+3}) & (-B_{j+2}\Gamma_{j+3}b_{j+3}) & 0\cdots \\
0 & 0 & (C_{j+4}w_{j+3}a_{j+3}) & \cdots & & & \\
\vdots & \vdots & (A_{j+4}w_{j+3}a_{j+3}) & \cdots & \text{etc.} & & \\
\vdots & \vdots & \vdots & & & &
\end{bmatrix}$$

Matrix **B** ($j=s$ or $j=s+1$)

Banded matrix with bandwidth 6. The underlined terms are equal to zero when $j=s$.

$$\begin{bmatrix}
(e_j) & (f_j-\underline{C_jw_{j-1}d_{j-1}}-D_jw_{j+1}c_{j+1}) & (0) & (-D_jw_{j+1}d_{j+1}) & (0) & \cdots \\
(f_j) & (e_j-\underline{A_jw_{j-1}d_{j-1}}+B_jw_{j+1}c_{j+1}) & (0) & (B_jw_{j+1}d_{j+1}) & (0) & \cdots \\
0 & (-C_{j+2}w_{j+1}c_{j+1}) & (e_{j+2}) & (f_{j+2}-C_{j+2}w_{j+1}d_{j+1}-D_{j+2}w_{j+3}c_{j+3}) & (0) & (-D_{j+2}w_{j+3}d_{j+3}) \\
0 & (-A_{j+2}w_{j+1}c_{j+1}) & (f_{j+2}) & (e_{j+2}-A_{j+2}w_{j+1}d_{j+1}+B_{j+2}w_{j+3}c_{j+3}) & (0) & (B_{j+2}w_{j+3}d_{j+3}) \\
0 & 0 & (\cdots) & \text{etc.} & & \\
\cdot & \cdot & 0 & & & \\
\cdot & \cdot & \cdot & & &
\end{bmatrix}$$

Eq. (C5) is multiplied by the inverse of matrix $\mathbf{A}$ to give

$$\dot{\mathbf{Y}}=\mathbf{CY}, \quad \text{where} \quad \mathbf{C}=\mathbf{A}^{-1}\mathbf{B}. \tag{C6}$$

When we put $\mathbf{Y}(t')=\exp(-i\sigma t')\mathbf{W}$ in (C6) we obtain

$$(\mathbf{C}-\sigma\mathbf{I})\mathbf{W}=0, \tag{C7}$$

which is an ordinary eigenvalue-eigenfunction problem for σ if ω, Λ, s and S are given. $\mathbf{I}$ is the unity matrix and σ is in general complex, i.e., $\sigma=\lambda+i\nu$, where ν is the exponential *growth rate* of the solution.

In order to solve (C7) it is necessary to truncate the matrix $\mathbf{C}$, the size of which is changed in order to obtain a good accuracy of the eigenvalue being sought. For most of the calculations we have used 30×30 elements of $\mathbf{C}$. The convergence of the desired eigenvalues was verified by comparison with those of 36×36 and 42×42 matrices with agreement of 10^{-9}. The convergence of the most unstable root near neutral stability is slower because the solutions oscillate more between $\mu=0$ and $\mu=1$ than for the unstable modes far from neutral stability. For these cases the accuracy was better than 10^{-6}.

Once the eigenvectors containing Θ_n^s and Ψ_n^s are obtained, we may compute the following variables:

ZONAL, MERIDIONAL, AND VERTICAL VELOCITIES

$$U1_n^s=-a^{-1}(1-\mu^2)^{-\frac{1}{2}}[sX_n^s-(n-1)(n-s)/(2n-1)(\Psi_{n-1}^s+\Theta_{n-1}^s)+(n+2)(n+s+1)/(2n+3)(\Psi_{n+1}^s+\Theta_{n+1}^s)]$$

$$U3_n^s=-a^{-1}(1-\mu^2)^{-\frac{1}{2}}[-sX_n^s-(n-1)(n-s)/(2n-1)(\Psi_{n-1}^s-\Theta_{n-1}^s)+(n+2)(n+s+1)/(2n+3)(\Psi_{n+1}^s-\Theta_{n+1}^s)]$$

$$V1_n^s=ia^{-1}(1-\mu^2)^{-\frac{1}{2}}[s(\Psi_n^s+\Theta_n^s)-(n-1)(n-s)/(2n-1)X_{n-1}^s+(n+2)(n+s+1)/(2n+3)X_{n+1}^s]$$

$$V3_n^s=ia^{-1}(1-\mu^2)^{-\frac{1}{2}}[s(\Psi_n^s-\Theta_n^s)+(n-1)(n-s)/(2n-1)X_{n-1}^s-(n+2)(n+s+1)/(2n+3)X_{n+1}^s]$$

$$\tilde{\omega}2_n^s=ia^{-2}\Delta pn(n+1)X_n^s.$$

The longitudinally average transports are computed using:

$$\overline{u_1'v_1'}=\tfrac{1}{2}\,\mathrm{Re}(\overline{U1'V1'^*})$$

$$\overline{u_3'v_3'}=\tfrac{1}{2}\,\mathrm{Re}(\overline{U3'V3'^*})$$

$$\overline{v_2'T_2'}=\tfrac{1}{2}\,\mathrm{Re}(\overline{V2'T2'^*})$$

$$\overline{\omega_2'T_2'}=\tfrac{1}{2}\,\mathrm{Re}(\overline{\tilde{\omega}2'T2'^*})$$

where the asterisks mean complex conjugate and $V2=(V1+V3)/2$.

a. Energetics of the models with $\delta=0$

An energy equation is obtained by multiplying (6.11)–(6.13) (with $\delta=0$) by Ψ, Θ and $2\tau/S$, respectively, and applying the operators

$$\bar{(\ )}\equiv\tfrac{1}{2}\int_0^{2\pi}(\ )d\phi \quad \text{and} \quad \langle(\ )\rangle\equiv\tfrac{1}{2}\int_{-1}^{+1}(\ )d\mu.$$

The result is

$$(\partial/\partial t')\langle\bar{E}\rangle=(1+2\gamma\omega)(\Lambda/S)\langle\overline{\mu\tau\partial\psi/\partial\phi}\rangle+\gamma\Lambda\langle(1-\mu^2)\overline{(\partial\psi/\partial\mu)\mathfrak{L}\chi}\rangle, \tag{C8}$$

where

$$2\langle\bar{E}\rangle=\langle\overline{(D(\Psi)^2+(D\Theta)^2+1/S\tau^2}\rangle \quad \text{and} \quad D\equiv a\nabla.$$

The unstable modes have $\partial/\partial t'<\bar{E}>>0$. For $\gamma=0$, the change in $\langle\bar{E}\rangle$ with time depends on the integral with respect to μ of the horizontal heat transport by the baroclinic eddies weighted by the horizontal basic temperature gradient. For $\gamma=1$ there is an additional vertical Reynolds stress term acting upon the vertical shear of the zonal basic flow that contributes to the increase (or decrease) of the perturbation total energy.

We can finally note that if $\Lambda=0$ (i.e., no vertical shear) $\partial/\partial t'\ \langle\bar{E}\rangle=0$. This means that the basic zonal wind profile $U\propto\cos(\text{lat})$ is stable with respect to barotropic disturbances.

REFERENCES

Bolin, B., 1955: Numerical forecasting with the barotropic model. *Tellus*, **7**, 27–49.

Bryan, K., 1959: A numerical investigation of certain features of the general circulation. *Tellus*, **11**, 163–174.

Burger, A. P., 1958: Scale consideration of planetary motions of the atmosphere. *Tellus*, **10**, 195–205.

Chapman, S., and R. S. Lindzen, 1970: *Atmospheric Tides*. Gordon and Breach, 200 pp.

Charney, J. G., 1955: The use of the primitive equations of motion in numerical prediction. *Tellus*, **7**, 22–26.

——, 1962: Integration of the primitive and balance equations. *Proc. Intern. Symp. Numerical Weather Prediction*, Tokyo, Meteor. Soc. Japan, 131–152.

——, 1973: Planetary fluid dynamics. *Dynamic Meteorology*, P. Morel, Ed., D. Reidel Publ. Co., 97–371.

Clark, J. H. E., 1970: A quasi-geostrophic model of the winter stratospheric circulation. *Mon. Wea. Rev.*, **98**, 443–461.

Cunnold, D., F. Alyea, N. Phillips and R. Prinn, 1975: A three-dimensional dynamical-chemical model of atmospheric ozone. *J. Atmos. Sci.*, **32**, 170–194.

Dikii, L. A., 1965: The terrestrial atmosphere as an oscillating system. *Izv. Atmos. Oceanic Phys.*, **1**, 275–286.

Eliassen, A., and E. Palm, 1960: On the transfer of energy in stationary mountain waves. *Geofys. Publ.*, **22**, 1–23.

Flattery, T. W., 1967: Hough functions. Tech. Rept. No. 21, Dept. Geophys. Sci., The University of Chicago, 175 pp.

Haurwitz, B., 1940: The motion of atmospheric disturbances on the spherical earth. *J. Marine Res.*, **3**, 254–267.

Hough, S. S., 1898: On the application of harmonic analysis to the dynamical theory of tides. Part II: On the general integration

of Laplace's dynamical equations. *Phil. Trans. Roy. Soc. London*, **A191**, 139–185.

Houghton, D., 1968: Derivation of the elliptic condition for the balance equation in spherical coordinates. *J. Atmos. Sci.*, **25**, 927–928.

Jeffreys, H. and B. S. Jeffreys, 1972: *Methods of Mathematical Physics*, 3rd ed. Cambridge University Press, 718 pp.

Kato, S., 1966: Diurnal atmospheric oscillations. *J. Geophys. Res.*, **71**, 3201–3214.

Korn, G. A. and T. M. Korn, 1968: *Mathematical Handbook for Scientists and Engineers*. 2nd ed. McGraw-Hill, 1130 pp.

Lamb, H., 1932: *Hydrodynamics*. 6th ed. Dover, 738 pp.

Leovy, C., 1964: Simple models of thermally driven mesospheric circulation. *J. Atmos. Sci.*, **24**, 327–341.

Lindzen, R. S., 1966: On the theory of the diurnal tide. *Mon. Wea. Rev.*, **94**, 295–301.

——, 1967: Planetary waves on beta-planes. *Mon. Wea. Rev.*, **95**, 441–451.

——, 1971: Atmospheric tides. *Lectures in Applied Mathematics*, Vol. 14 Amer. Math. Soc., 293–362.

Longuet-Higgins, M. S., 1968: The eigenfunctions of Laplace's tidal equations over a sphere. *Phil. Trans. Roy. Soc. London*, **A262**, 511–607.

Lorenz, E. N., 1960: Energy and numerical weather prediction. *Tellus*, **12**, 4, 364–373.

Maruyama, T., 1967: Large-scale disturbances in the equatorial lower stratosphere. *J. Meteor. Soc. Japan*, **46**, 391–408.

Matsuno, T., 1966: Quasi-geostrophic motions in the equatorial area. *J. Meteor. Soc. Japan*, **44**, 25–42.

Miyakoda, K., 1960: Numerical solution of the balance equation. Tech. Rept. JMA No. 3, Japan Meteor. Agency, Tokyo.

Monin, A. S., 1952: Changes of pressure in a barotropic atmosphere. *Izv. Akad. Nauk. SSSR, Ser. Geofiz.*, **4**, 76–85.

——, 1958: Pressure variations in a baroclinic atmosphere. *Izv. Akad. Nauk. SSSR Ser. Geofiz.*, **4**, 280–286.

Moura, A. D., 1974: The eigensolutions of the balance equations over a sphere. Doctoral dissertation, Massachusetts Institute of Technology, 171 pp.

——, and P. H. Stone, 1975: The effects of spherical geometry on baroclinic instability. *J. Atmos. Sci.* (to be published).

Oort, A. H., and E. M. Rasmusson, 1971: Atmospheric circulation statistics. NOAA Prof. Paper 5, 323 pp. [Available from Govt. Printing Office, Stock No. 0317-0045, C55.25: 5].

Peng, L., 1965: A simple numerical experiment concerning the general circulation in the lower stratosphere. *Pure Appl. Geophys.*, **61**, 191–218.

Phillips, N. A., 1954: Energy transformations and meridional circulations associated with simple baroclinic waves in a two-level, quasi-geostrophic model. *Tellus*, **6**, 273–286.

——, 1960: On the problem of initial data for the primitive equations. *Tellus*, **12**, 121–126.

——, 1963: Geostrophic motion. *Rev. Geophys.*, **1**, 123–176.

——, 1973: Principles of large scale numerical weather prediction. *Dynamic Meteorology*, P. Morel, Ed., D. Reidel Publ. Co. 1–96.

Rossby, C. G., 1939: Relation between variations in the intensity of the zonal circulation of the atmosphere and the displacement of the semi-permanent centers of action. *J. Marine Res.*, **2**, 38–55.

Taylor, G. I., 1936: The oscillations of the atmosphere. *Proc. Roy. Soc. London*, **A156**, 318–326.

Wallace, J. M., 1971: Spectral studies of tropospheric disturbances in the tropical western Pacific. *Rev. Geophys. Space Phys.*, **9**, 557–612.

——, and V. E. Kousky, 1968: Observational evidence of Kelvin waves in the tropical atmosphere. *J. Atmos. Sci.*, **25**, 900–907.

Webster, P. J., 1972: Response of the tropical atmosphere to local, steady forcing. *Mon. Wea. Rev.*, **100**, 518–541.

Yanai, M., and T. Maruyama, 1966: Stratospheric wave disturbances propagating over the equatorial Pacific. *J. Meteor. Soc. Japan*, **44**, 291–294.